Environmental triggers of faunal changes revealed by benthic foraminiferal monitoring

Joachim Schönfeld[a*], Isabel Mendes[b]

[a]GEOMAR Helmholtz Zentrum für Ozeanfoschung Kiel, Wischhofstrasse 1-3, 24148 Kiel, Germany.
[b]Centro de Investigação Marinha e Ambiental (CIMA), Universidade do Algarve, Campus de Gambelas, 8005-139 Faro, Portugal.
* Corresponding author. E-mail address: jschoenfeld@geomar.de

Abstract

Benthic foraminifera are deemed sensitive indicators of environmental conditions. Triggers and magnitudes of faunal response to environmental changes are yet poorly constrained. Benthic foraminiferal faunas were monitored annually at Ria Formosa (Algarve, Portugal) coastal lagoon since 2013. Distinct environmental changes were recognised during the monitoring period. The relocation of a tidal inlet in winter 2015 effected faster flushing, higher tidal levels, and stronger currents in the Esteiro do Ancão tidal channel. The epibenthic foraminiferal species *Asterigerinata mamilla* increased in abundance and the population densities of the whole fauna were double as high as before inlet relocation. Enhanced sediment redeposition was recorded and extensive polychaeta colonies successively replaced firmground patches with oysters. The standing stock of the foraminiferal fauna declined in the next year due to food impoverishment, while the high hydraulic energy levels and high percentages of *Asterigerinata mamilla* maintained. Benthic foraminifera responded much faster to environmental perturbations than macroorganisms identifying them as powerful proxies in environmental studies.

1. Introduction

The earth's climate and ocean circulation were thought to have changed in a cyclical manner between Glacials and Interglacials during the Pleistocene (Nilson, 1983). The transitions were deemed to have taken several thousand years, allowing marine and terrestrial biota to pursue migratory responses with sufficient time (e.g. Lutze et al., 1979). The investigation of high resolution climate archives revealed, however, that climatic variations rather show a saw-tooth than sinusoidal pattern (Dansgaard et al., 1993). The switch to a new state happened during a short period while the return to conditions that prevailed before took rather long.

One reason for this asymmetric pattern is the excess of certain threshold values. The excess may cause irreversible changes in ocean circulation and climate (Lenton et al., 2008; Solomon et al.,

Accepted for publication in Estuarine, Coastal and Shelf Science [YECSS_107313] *4-March-2021*

2009). Such changes may happen within periods of less than a decade (Lenton et al., 2019; Steffensen et al., 2008). The return to previous conditions may be subjected to a hysteresis pattern, as for instance the lagged resumption of thermohaline circulation in the northern Atlantic, after excess freshwater influx during Heinrich Events (Alley et al., 1993; Bond et al., 1993; Manabe and Stouffer, 1988, 1997; Rahmstorf, 1994; Taylor et al., 1993; Zahn et al., 1997). Despite vegetation changes (e.g. Mayle and Cwynar, 1995; Paus, 1989; Roucoux et al., 2001), the complex response pattern of marine biota to sudden environmental changes in the geological past has received little attention (e.g. Schönfeld et al., 2003).

The accelerated rise in atmospheric CO_2 levels and temperatures during the last decades stimulated research on the resilience and adaptation of marine plankton and benthic macrofauna to ocean warming and acidification (e.g. Cantin et al., 2010; Hughes et al., 2017; Kleypas et al., 1999; Riebesel et al., 2000). Surprisingly, evolutionary adaptation and migration were recognised as the main adaptive strategies. They involve many generations, which makes it difficult to cope with Global Change or weather extremes (e.g. Harvey et al., 2014; Miller et al., 2017).

Among marine biota, foraminifera have rather short generation times of 14 days to 2 years (Boltovskoy and Wright, 1976). They occur in all marine environments in large numbers and their tests are readily preserved in the fossil record. Therefore, foraminifera are widely used as proxies in both, Recent and palaeo-environmental studies (e.g. Mojtahid et al., 2009; Bouchet et al., 2012; Dolven et al., 2013; Duffield et al., 2015; Mendes et al. 2013; Nordberg et al., 2017; Polovodova Asteman and Nordberg, 2013). Only a few laboratory experiments unveiled the response pattern of certain species or assemblages to the deterioration of environmental parameters such as temperature, salinity, oxygen, food supply and trace-metal pollution (Alve and Bernhard, 1995; Altenbach, 1992; Elderfield et al., 2006; Havach et al., 2001; Le Cadre and Debenay, 2006). Some of these experiments were anticipatory to future scenarios of Global Change, others mirrored impact levels far beyond any observed or expected natural conditions, in particular to better constrain proxy calibration functions (e.g. Wit et al., 2013).

Long-term foraminiferal monitoring studies or investigations of high-resolution sediment archives offer the opportunity to assess faunal responses to environmental changes in their natural ecosystems. The few studies reveal that foraminiferal response happens very fast, or with a delay of some years due to the accumulation of empty tests in the sediment (e.g. Mendes et al., 2020; Schönfeld, 2018).

The purpose of the present paper is to obtain a better understanding of the response pattern of benthic foraminifera to environmental perturbations. The following hypothesis is to be tested: once a limiting environmental variable exceeds a certain threshold, the foraminiferal assemblage will change to a new state. The faunal composition and density will not bounce back, once the respective variable returns to the conditions that prevailed before. At Ria Formosa coastal lagoon the Esteiro do Ancão foraminiferal time series was investigated to test this hypothesis.

1.1 Geographical and environmental setting

Ria Formosa is a large coastal lagoon with a surface area of 105 km^2 and 2 m average depth. It is connected to the adjacent ocean in the Gulf of Cadiz by six broad inlets between five barrier islands and two peninsular spit bars, facilitating an almost complete water exchange during each tidal cycle (e.g. Pacheco et al., 2010; Rosa et al., 2019; Tett et al., 2003). The lagoon is dominated by sand or mud flats, patchy salt marshes and a dense, complex network of channels, of which Esteiro do Ancão is one of the major tributary and serves the remote, northwestern part of Ria Formosa (Fig. 1) (Andrade et al., 2004). Esteiro do Ancão was occasionally dredged, and the bottom is covered with a sandy gravel lag. The channel is bounded by a series of shallow mud banks covered with sea grass (*Zostera noltii*), which pass into extended sand flats to the Northeast. On the southwestern side of the channel, the mud banks are cut by runnels at the foot of the steep slope of Ancão Peninsula backbarrier sandy beach. The salinities and water temperatures ranged from 15 to 39 units and 9 to 30°C in the western part of Ria Formosa lagoon, with high temperatures and salinities during summer (Barbosa, 2010). The tides are semidiurnal, the average amplitude is 2.8 m, during spring and 1.3 m during neap-tides (Pacheco et al., 2010).

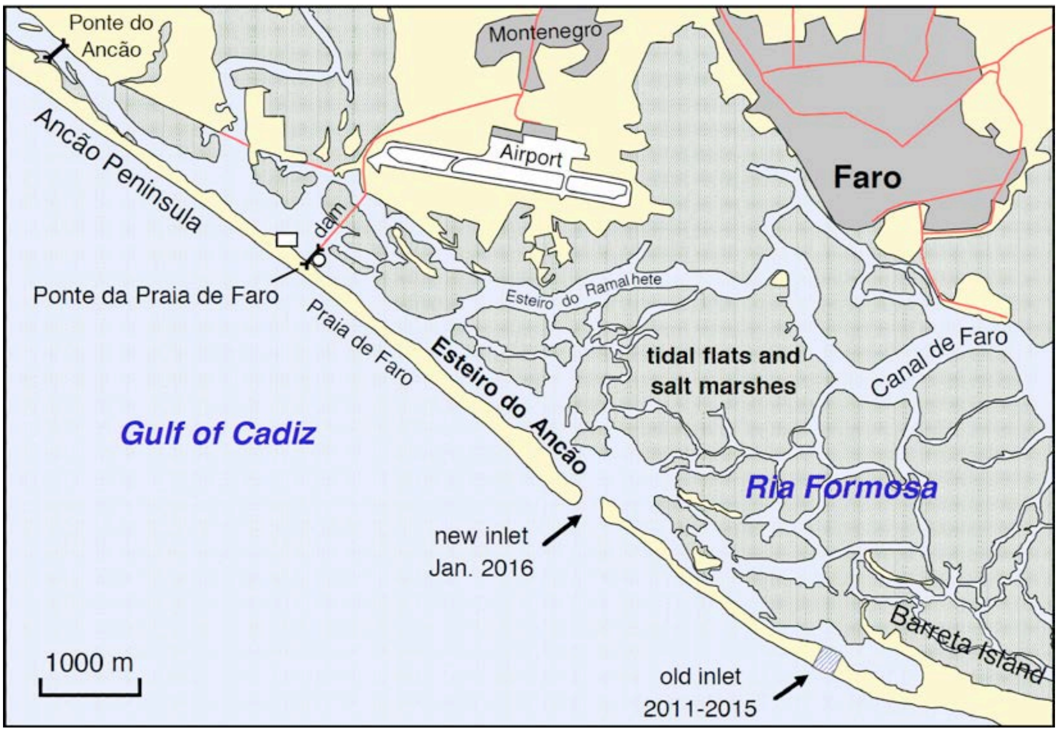

Fig. 1. Geography of the study are. Grey: urban areas, red lines: main roads and dams, square: monitoring site (Fig. 2), circle: tide gauge and hydrographical measurements. Redrawn after Carta Militar de Portugal, Folha 610, 611, © Instituto Geográfico do Exército, Lisboa, 2006.

The northwestern Ria Formosa saltmarshes are disconnected by a dam (road) and Ponte da Praia de Faro, the bridge to Praia de Faro, crossing Esteiro do Ancão (Fig. 1). In winter 2015, two new conduits were built under the dam and the Ancão inlet was relocated ca. 2.9 km to the Northwest on the peninsula (Jacob and Cravo, 2019). These measures were intended to effect a faster tidal flushing and hence better drainage and ventilation of the northwestern Ria Formosa intertidal area. The same relocation has been done in 1997 (Andrade et al., 2004; Dias et al., 2009), and, as the inlet is drifting with ca. 20 to 40 m yr^{-1} to the southeast (Pacheco et al., 2007), it will probably be necessary again in the near future.

Furthermore, extensive construction works were pursued in spring 2015. Unauthorised settlements were cleared on Ancão Peninsula and in the salt marshes of the northwestern Ria Formosa, and other anthropogenic debris was collected, mainly floating plastics. There was intense traffic of earth work vehicles all around the area, on the backbarrier beach and in the salt marshes, and a mobile platform was hauled to Esteiro do Ancão and berthed at Ancão Peninsula to the Southeast of the bridge.

1.2 Foraminiferal assemblages

Benthic foraminiferal assemblages were scarcely studied at Ria Formosa. There is only one publication reporting thirty-seven foraminiferal species or groups recorded in four surface sediment samples from western Ria Formosa channels (Andrade et al., 2004). The authors stated that rose-Bengal stained, living specimens were too sparse for a sound assessment of the living fauna. None-the-less, *Textularia earlandi, Reophax* cf. *curtus, Ammonia tepida* and *Discorbis* spp. were found, the latter two with high abundances. *Haynesina germanica* and *Planorbulina mediterranensis* were frequent in the dead assemblages.

2 Material and methods

The foraminiferal time series from Esteiro do Ancão tidal channel at Ria Formosa (Algarve, Portugal) was established in 2013 and sampled annually in late April to early May. Bloom periods are to be avoided when sampling for monitoring studies (Schönfeld et al., 2012). Therefore, we have chosen the short interval between enhanced benthic macroalgae growth in winter, ranging from October to April (Sprung, 1994), and the plankton summer bloom that usually occurs from May to September in the study area (Barbosa, 2010; Galvão et al., 2019). Sampling was skipped in spring 2020 due to the Covid-19 pandemic travel ban. A 45-m long beach transect from the spring high-water line to the middle of a mud bank, heading to 36°N was investigated on each sampling campaign (Fig. 2). The height of the sediment surface was determined at 2 – 3 m intervals along the transect with a Leica

NA728 surveyor's level. The levels were tied to the geodetic reference points IHBH 29/99 at the bus turn on the dam (2.660 m) and DGP MBH4 on the bridge platform (3.291 m). The accuracy of levelling is < ±0.4 cm. All levels were referred to the Portuguese Ordnance Datum (nível médio adotado, POD).

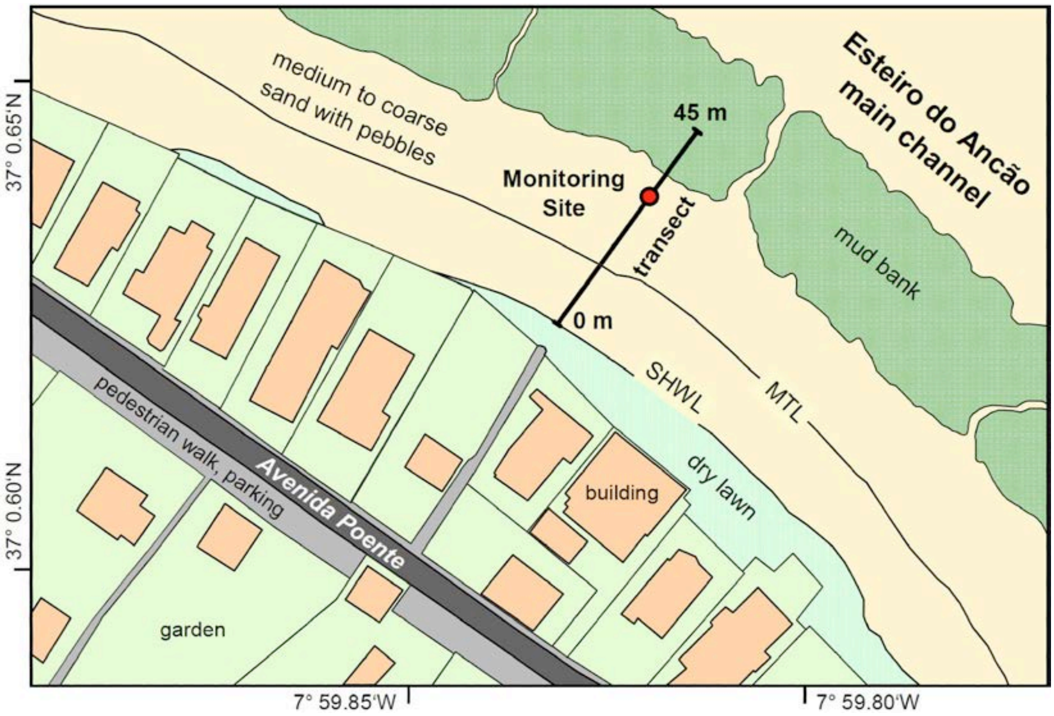

Fig. 2. Location map of the monitoring site and transect investigated on Esteiro do Ancão backbarrier beach of Ancão Peninsula. MTL: mean tidal level, SHWL: highest spring high water line, red dot: monitoring site at 30m. The map was drawn after satellite images and personal observations.

Sediment composition, structures, facies boundaries, macroorganism and macrophyte occurrences were recognised, described and measured along the transect in order to assess annual changes, also with reference to erosion and mudbank accretion. The descriptions were performed by two persons in order to minimize individual bias. Additionally, the halophytic flora was inspected annually in the salt marsh immediately to the North of the dam to Praia de Faro (Fig. 1).

Foraminiferal samples were taken at the 30-m monitoring site at 37°0.639'N and 7°59.819'W (Fig. 2) from 2013 to 2019, because it represents a unique habitat. A varying number of supplementary samples were taken along the transect at distances of 2 – 5 m, of which the series of 2014 through 2017 were analysed and considered in the present study. The exact sample position was chosen according to sedimentary structures and macrofauna occurrences. A polycarbonate tube of 54 mm inner diameter (28.5 mm in 2013), a graduated plastic ring of the same diameter, and a shuffle spatula was used to detach the uppermost 1 cm of the sediment following Schönfeld et al. (2012). Pebbles or shell fragments often obstructed the spatula leading to higher or lower sample volumes than expected. The samples were transferred into 100 mL PVC (Kautex$^{®}$) bottles. Due to the inhomogeneous sediment texture and irregular sample surface, it was often not possible to mark the sediment volume on the vial in the field with appropriate accuracy. The samples were preserved and stained with a rose Bengal solution of 2 g in 1 l vodka (40 %) for shipment as non-dangerous substance (Schönfeld 2012). Alcohol and stain was exchanged after transport, and the ethanol concentration was raised to >90 % for long-term storage, i.e. several months or more.

The samples were prepared and analysed following the procedures described by Wefer (1976), Schönfeld et al. (2013) and Lübbers and Schönfeld (2018). The 63-2000 µm size fraction was wet picked completely for well-stained foraminifera that were living at the time of sampling (Lutze and Altenbach, 1991), including those that were still attached to large sand grains. Aliquots containing approximately 100–300 living specimens were made with a Motodo wet splitter when necessary. After the living forms were sorted out, the residues or aliquots were dried and weighed. The splits of samples from the 30-monitoring site were subsequently picked for dead foraminifera. Aliquots with ca. 200–250 specimens were made with a Green Geological microsplitter when necessary. The exact split ratio was calculated from the weights of the aliquots. The picked individuals from the living faunas and dead assemblages were each sorted by species in separate Plummer cell slides, fixed with glue, and counted. Epifaunal specimens living at the time of sampling were scraped off from their substrate if that was too large for the cell slide. Images for species' documentation were taken with a Keyence VHX-7000 digital microscope at the Institute of Geosciences, Kiel University. Faunal indices were calculated with Past v3.16 (Hammer et al., 2001).

Hydrographic measurements include the installation of a temporary tide gauge at Ponte da Praia de Faro during the sampling campaigns in 2013 through 2017. The water level and temperature of Esteiro do Ancão was measured at 5 (2013 only) or 10-minutes intervals with Odyssey pressure–temperature recorders. Between 5 and 23 tidal cycles were recorded. The height of the pressure sensor was levelled and tied to the geodetic reference point DGP MBH4 on the bridge. The sensor accuracy after calibration was ±0.29 cm for immersion depth and ±0.23°C for temperature (1-sigma values; Schönfeld, 2018). The water level measurements were compared with forecasts of Instituto Hidrográfico tide table 201.12, Barra de Faro-Olhão, and the X-Tide astronomical model (https://tides.mobilegeographics.com/locations/2459.html, WXTide32 program for Windows).

Current meter casts were performed at the main conduit (navigation channel) of Ponte da Praia de Faro during the tide gauge logging periods in 2014, 2015 and 2017 (Fig. 1). The hydrocasts were performed from the bridge every hour during a half or complete tidal cycle. Velocities, temperatures and salinities were measured at three depths with a General Oceanics Model 2030 R flowmeter mounted to a custom-made CTD, with Odyssey pressure–temperature and conductivity–temperature recorders or a TetraCon 325 temperature–conductivity probe (2017 only). A concrete or limestone depressor was used with weights of 2.5, 7.2 and 5.1 kg respectively. Rope length and inclination was recorded on each deployment. This setting facilitated the calculation of both, immersion depths and heights of flow meter, temperature and conductivity probes. The accuracy of the Odyssey conductivity sensors after calibration with standard solutions was ±0.18 salinity units, the accuracy of the TetraCon 325 probe was ±0.13 units (1-sigma values). For the flow meter, manufacturer's charts were used to estimate current velocity from counts, i.e. 1/10 revolutions per second. The accuracy of General Oceanics 2030 R flowmeters was in the range of 1.0 to 6.2, on average 3.1 % difference of the measured value to the reference flow speed (Potter, 1978: Table 2).

Salinity and temperature of Esteiro do Ancão ebb waters were routinely measured during the sampling campaigns with hand-held WTW Cond 3210 or LF320 conductimeters equipped with a TetraCon 325 probe. The conductimeters had a precision of < 0.5 % of measured conductivity and < 0.1 K according to a manufacturer's test certificate (Schönfeld, 2018). Water samples were taken from ebb waters in winter 2016/2017, and during the sampling campaigns in 2017, 2018 and 2019. They were syringe filtered (200 nm), 18 - 20 cm^3 were transferred into cleaned HDPE Zinser vials, kept on ice for transport and were frozen after ten hours at maximum. The samples were transported to Kiel in a frozen state and later analysed for nitrite, nitrate and phosphate concentrations by using standard methods (https://www.geomar.de/en/mg-analytik).

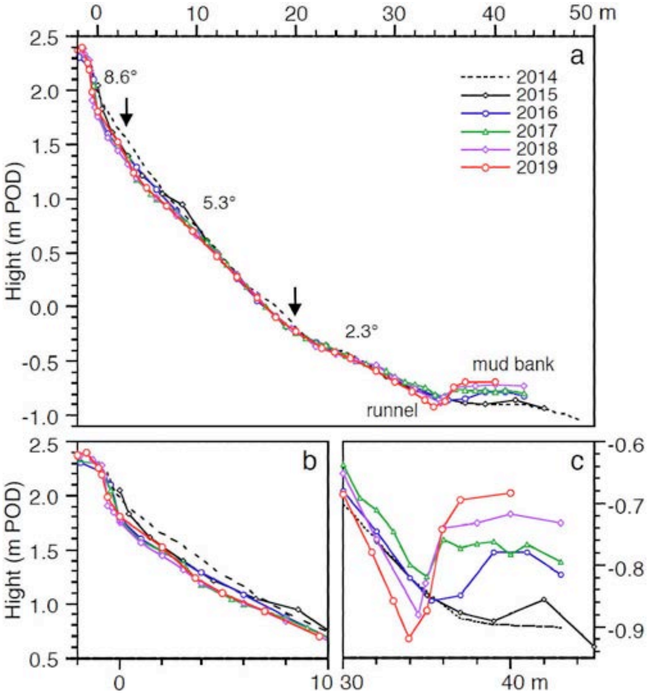

Fig 3. Morphology of the backbarrier beach transect from 2014 through 2019 (a). Arrows: hinge points of changing slope angle. The bottom panels show the set back of the brink at transect zero and erosion in the uppermost part of the transect (b), and the incision of the runnel and accretion of the mud bank (c).

3 Results

3.1 Morphology, sedimentary and biogenic structures

Ancão Peninsula backbarrier beach transect at Esteiro do Ancão commences at 37°0.626’N and 7°59.832’W. In this area a small brink separates the supratidal platform with dry lawn vegetation on medium sand from a pervasive debris seam depicting recent spring high water levels at 1.81 m POD (Fig. 2). The brink at transect zero was set back by 1.2 m in 2016, after the new conduit has been built (Figs. 3a, b).

A steep slope with an angle of 8.6° follows, which was covered with medium sand and showed temporary debris seams and patchy heavy mineral placers (Supplement Table 1). A brown, lithified saltmarsh peat was outcropping here as well. The sediment passed into a coarse sand with pebbles and shell debris around 3 m in section and 1.3 m POD, where the average slope angle decreases to 5.3°. The level corresponds to Mean High Water. The change in sediment composition may vary from 2.3 to 4.2 m, and even was recognised at 6.5 m in 2016. Well-sorted coarse sand or pebble bands on the surface forming water level marks were common (Supplement Table 1). The lower boundary of water level marks was 14.3 to 15 m before, and 16 to 19.1 m after the new conduit has been built. Flute marks and small current ripples were occasionally recorded. A further coarsening and increase in pebble content was recognised beyond the water level marks. Ginko-leaf shaped megaripples of 60 x 80 cm dimension and up to 10 cm hight were common before 2016. Thereafter, only irregular undulations of the surface prevailed. They were intersected by dewatering rills commencing in small seep pits. Scattered, small *Ulva* was common, green algae and gastropods (*Littorina*) were occasionally found. The lower boundary of this unit at 19 – 21 m did not change during the investigation period. A hinge in slope angle was recognised here at 20 m and -0.28 m POD, which was 2.3° on average.

Medium to coarse sands with varying contents of pebbles and shell debris was found in the next unit (Supplement Table 1). A marked feature were elongated, oval firmground patches of 0.1 – 0,2 to 1 – 3 m in size and 3 – 5 cm hight. They were based on agglomerations of pebbles and shells, stabilized by sepulids, balanids, hydroids, and overgrown by small oysters, tunicates and sea anemones. Gastropods were also recorded, littoral crabs and hermit crabs were common. Large *Ulva* were rooted on the firmgrounds. Their leaves entirely covered the agglomerations during emergence time. Firmground occurrences were variable before 2016, between 22.5 and 36 m. They remained between 21 and 35 m in 2016, and between 19.1 and 26.8 m in 2017 though much smaller in size. Cluster of densely-packed polychaeta tubes established in 2016 between 26 and 34 m. These colonies were 0.2 – 0.7 m in diameter. However, the dimensions were difficult to assess as the polychaets tend to inhabit patches of medium sand, in which they hide. In 2018 and 2019, *Ulva* is rooted on large pebbles, which are loosely colonized by barnacles, serpulids, and hydroids.

The next unit was a muddy coarse sand, covered with a shell and pebble lag in places, which developed as a gutter before the aggrading mud bank (Fig. 3c). This unit prevailed between 32 and 38 m before 2016, and tapered to a 1.2 m wide runnel thereafter. Barnacles, hydroids, and *Ulva* were common, hermit crabs and small *Bittium* gastropods were frequent. The mud bank commenced at 37 – 38 m in 2013 through 2015, and at 36 – 35 m after the new conduit has been built. The bank is silting up with 4.6 cm yr^{-1} on average, while the runnel incised. The surface sediment was a sandy to clayey mud. The bank was covered with a dense seagrass meadow (*Zostera noltii*). Sponges, tunicates, and patches of filamentous green algae were common, sea cucumbers, hermit crabs and gastropods were occasionally recorded.

3.2 Hydrography

Salinity and temperatures of Esteiro do Ancão waters ranged from 34.4 to 37.1 units and 17.0 to 25.7°C, with mean values of 36.1 and 20.1°C in late April to early May 2013 through 2019. Incoming flood waters were with 35.8 units on average slightly lower in salinity than ebb waters with 36.4 units (Supplement Table 2). No systematic change in salinity or temperature was recognised after relocation of the Ancão inlet in winter 2015.

The Mean Tidal Level was estimated to 0.34 m POD (Supplement Table 3). It was 0.29 m POD (n = 41 tidal cycles, weighed mean) before relocation of the Ancão inlet and 0.41 m POD thereafter (n = 30 tidal cycles, weighed mean). The mean flood period was 6:20 h before and 6:27 h after relocation. Correspondingly, the mean ebb period shortened from 6:00 before to 5:55 h after inlet relocation. The tide gauge records mainly cover periods around spring tides, and they were too short to determine average tidal amplitudes, high water or low water levels with a sufficient accuracy. None-the-less, the differences of observations and predictions could be assessed. The High Tide levels were higher on average by 0.25 m than predicted before relocation of the inlet and 0.45 m thereafter. The Low Tide levels were higher on average by 0.19 m than predicted before and after conduit relocation, hence did not change. The average time lag between observation and prediction shortened from 0:52 to 0:31 h for High Tides and from 1:00 to 0:33 h for Low Tides after inlet relocation.

The tidal curves of the 5th High Tide after New Moon 4 to 7, between 12th April and 8th May, were assessed during the monitoring periods in 2013, 2014, 2016 and 2017. The tidal curves showed an ebb-skewed triangular shape and rather compare to a linear than sinusoidal, astronomical model (Fig. 4a). The shape of the curves did not substantially change after inlet relocation. Half-range flood was attained at 2:57 h after low tide before, and 2:51 h after low tide after inlet relocation, whereas half-range ebb was 9:55 h after low tide before and 9:57 h after low tide after relocation. These differences account for an increase in submergence time by 8 minutes or 2 % at Mean Tidal Level after inlet relocation. It was mainly achieved during the later part of the flood period as indicated by the differences of the tidal curves to the linear or astronomical model (Figs. 4b, c).

The current velocities in Esteiro do Ancão were rather uniform in upper and middle part of water column at Ponte da Praia de Faro (Fig. 5a). A transient tiering was recognised. The velocities markedly decreased by 2/3 of the values at ca. 1 – 1.5 m above the channel bottom. The near-bottom velocities may increase to 1/2 of the values above during the mid of flood and ebb periods. The slack water intervals at High or Low Water were with ca. 30 minutes rather short. Ebb currents were generally stronger than flood currents and may reach peak values of 0.9 m s^{-1}. The average current velocities during ebb and flood periods were offset by ca. 0.1 to 0.15 m s^{-1} (Supplement Table 4). A significant correlation with the tidal amplitude was recognised for both, mean ebb and flood currents (r = 0.89, 0.97; p = 0.06, 0.02) (Fig. 5b). A covariance of maximum current velocities during each 1/2 tidal cycle with tidal amplitude was also recognised. The data showed more scatter than the mean velocities. Inflow and outflow data were less separated. Measurements taken in 2017 after the inlet relocation showed no different pattern than the other data from current measurements in 2014 or 2015 (Figs. 5b, c).

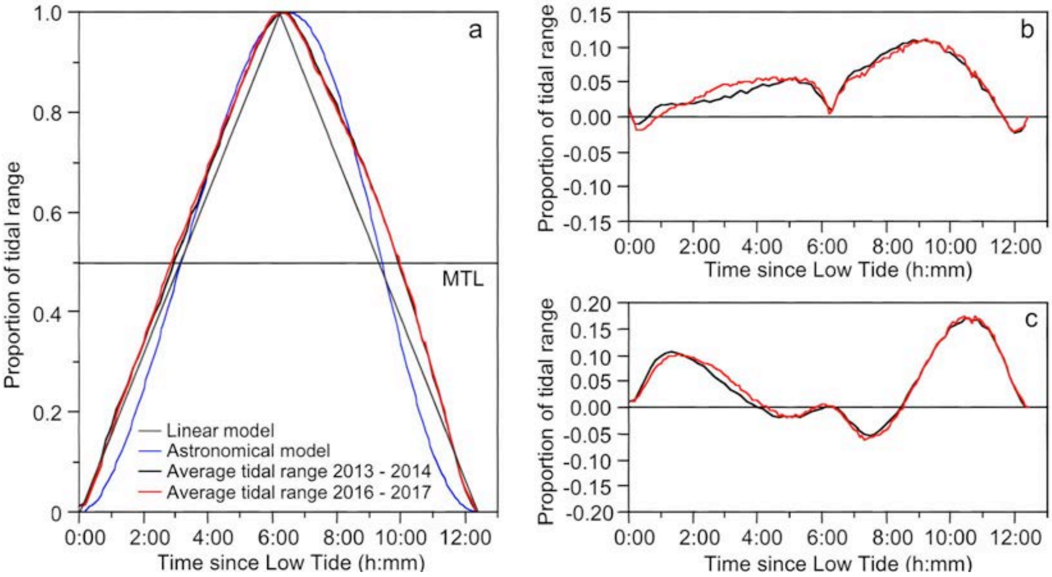

Fig. 4. Tidal curves at Ponte da Praia de Faro of the 5th High Tide after New Moon 4 to 7, 12th April to 8th May, from 2013 to 2017. Panel a: comparison of the measured tidal curves with the linear and astronomical model. MTL: mean tidal level. Panel b: difference to the linear model (thin black line in panel a). Panel c: difference to the astronomical model (blue curve in panel a). The average tidal curves after inlet relocation are given in red.

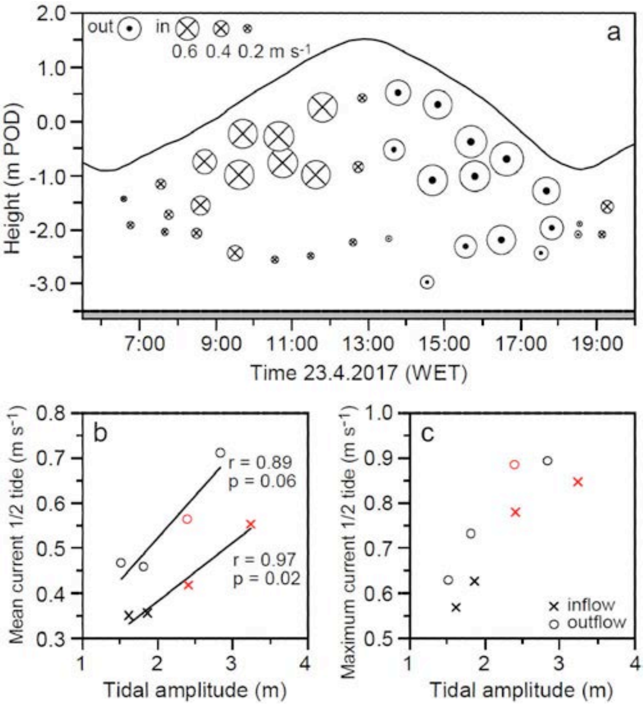

Fig. 5. Current measurements at Ponte da Praia de Faro during a full tidal cycle (a). Mean (b) and maximum current velocities (c) measured during a flood or ebb period versus tidal amplitude. Red symbols: hydrocasts after inlet relocation.

3.3 Living benthic foraminifera

At Esteiro do Ancão backbarrier beach transect, 105 different living foraminiferal species were recorded (Appendix 1, Plate 1). The majority of 51 species were rotaliids, 34 species were textulariids and 20 species were miliolids. The most abundant species were *Asterigerinata mamilla, Bolivina ordinaria, Bolivina striatula, Deuterammina balkwilli, Haynesina depressula, Quinqueloculina seminulum, Rosalina globularis* and *Rosalina vilardeboana*. Taxa with an attached mode of life were common, e.g. *Rosalina* spp. and Trochamminids. Species occurring on continental shelves at low to mid latitudes, e.g. *Rectuvigerina phlegeri*, *Bolivina ordinaria, Bolivina tongi*, *Lenticulina atlantica* and the meroplanktonic *Bolivina variabilis* were occasionally frequent in places. Species known from Nordic fjords, e.g. *Reophax nana*, *Reophax arctica* or *Ammoscalaria runiana*, were found as well. Foraminifera that were elsewhere common in salt marshes or on tidal flats, e.g. *Elphidium williamsoni, Haynesina germanica, Jadammina macrescens, Miliammina fusca* and *Trochammina inflata* were rare in the Esteiro do Ancão backbarrier intertidal zone. The eight most frequent species comprised on average 47 to 69 % of the living fauna in the upper and middle part of the transect, and 27 to 54 % in samples beyond 31 m. The individual proportions of the eight-ranked species ranged from 0.2 to 100 %, the averages varied form 8.2 % in 2017 to 15.7 % in 2016. The other species were markedly less abundant. They usually showed 0.5 to 5 %. Only a few of them were more frequent in places.

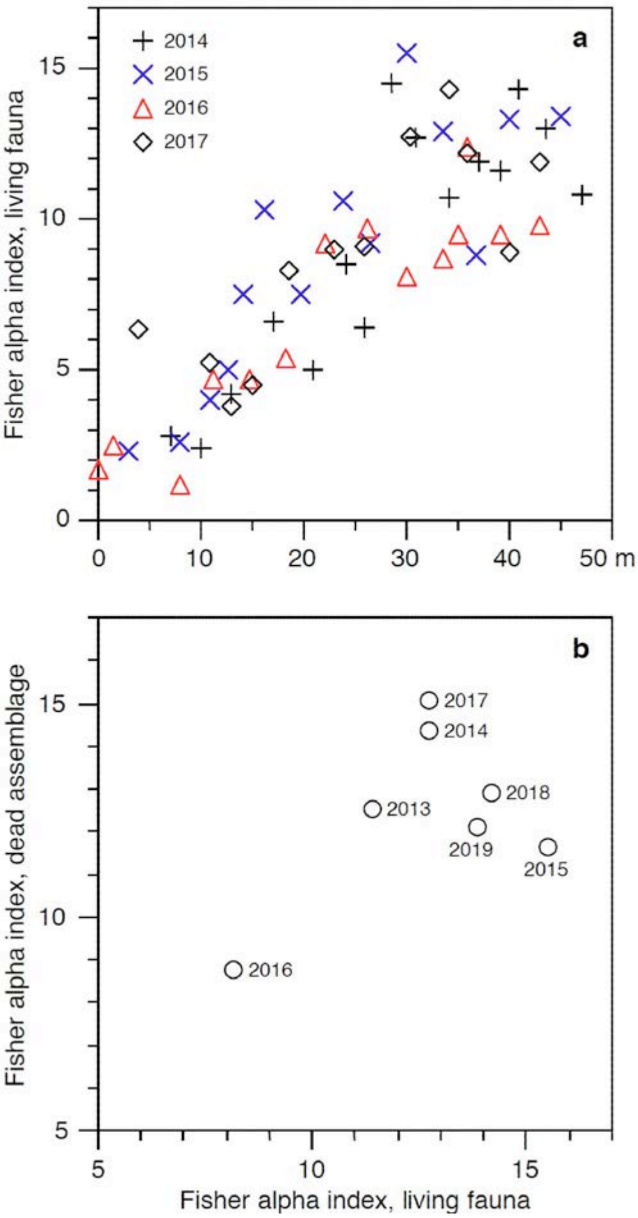

Fig. 6. Foraminiferal diversity distribution on the Esteiro do Ancão transect.

The Fisher alpha diversity indices ranged from 1.2 to 14.6 and showed low but variable values from transect zero to 10 m and a level of 0.73 m POD (Fig. 6a). The diversity index values and their scatter successively increased up to 30 m and -0.67 m POD, where the highest diversities were recorded. The values slightly decreased and their scatter diminished beyond 34 m and -0.8 m POD. There were no systematic offsets in diversity patterns between the years despite consistently lower Fisher alpha index values beyond 30 m in 2016.

The changes in diversity patterns are also mirrored in the structure of benthic foraminiferal faunas (Fig. 7, Supplement Tables 5 – 8). Samples from the upper and landward transect part showed high proportions of *Deuterammina balkwilli* and *Rosalina globularis*, the latter is dominant in 2015 and 2016 until 10 m, whereas *D. balkwilli* is dominant below until 15 m. *Haynesina depressula,*

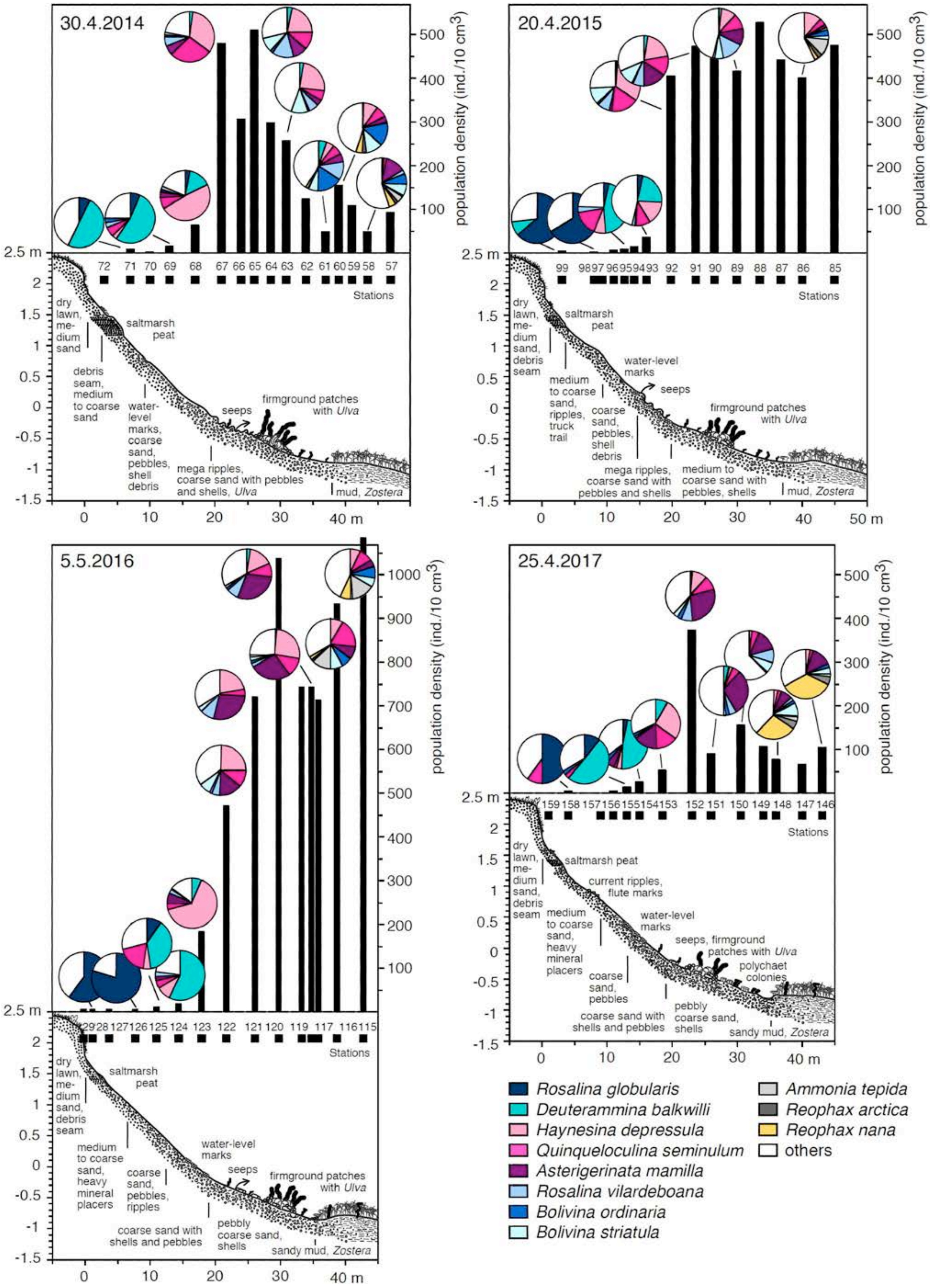

Fig. 7. Morphology, sediments, foraminiferal population densities and abundance of the eight-ranked and other common species along the Esteiro do Ancão transect.

Plate 1. Living (rose-Bengal stained) foraminifera from Esteiro do Ancão backbarrier beach, Ria Formosa, Algarve, Portugal. 1: *Eggerelloides scaber* (Station 57). 2, 3: *Ammoscalaria runiana*, 2 lateral view, 3 side view (Station 59). 4: *Jadammina macrescens*, ventral view (Station 128). 5: *Miliammina fusca* (Station 115). 6: *Reophax arctica* (Station 57). 7: *Reophax nana* (Station 59). 8: *Cornuspira involvens*, lateral view (Station 115). 9–12: *Deuterammina balkwilli*, 9 and 11 dorsal, 10 and 12 ventral view (Stations 69, 93). 13: *Quinqueloculina seminulum* (Station 120). 14, 15: *Rectuvigerina phlegeri* (Station 150). 16: *Bolivina ordinaria* (Station 57). 17: *Bolivina striatula* (Station 57). 18: *Bolivina variabilis* (Station 119). 19: *Bolivina*

tongi (Station 122). 20: *Haynesina germanica*, lateral view (Station 115). 21, 22: *Haynesina depressula*, lateral view (Station 68). 23: *Elphidium williamsoni*, lateral view (Station 68). 24–26: *Asterigerinata mamilla*, 24 side view, 25 dorsal, 26 ventral view (Station 120). 27: *Lenticulina atlantica*, lateral view (Station 120). 28–30: *Rosalina vilardeboana*, 28 ventral, 29 side view, 30 dorsal view (Station 119). 31–35: *Rosalina globularis*, 31 ventral, 32 dorsal view (juvenile specimens, Station 68), 33 ventral, 35 dorsal view (Station 129), 34 side view (Station 155). The locations of the individual stations on the transect are indicated on Figure 7.

Quinqueloculina seminulum and *Rosalina vilardeboana* showed successively increasing proportions from 15 m onwards while *D. balkwilli* and *R. globularis* declined. The first three dominated the assemblages together with *Asterigerinata mamilla* and *Bolivina striatula* in the middle part of the transect until ca. 35 m. The proportions of *Haynesina depressula, Quinqueloculina seminulum* and *Rosalina vilardeboana* decreased while the *Bolivina* species, in particular *B. ordinaria* increased in abundance beyond 35 m. *Ammoscalaria runiana, Eggerelloides scaber, Reophax arctica* and *Reophax nana* were common on the mud bank. Systematic, interannual changes in the faunal composition was the increase in abundance of *A. mamilla* in 2015, with maximum values in 2016. *Ammonia tepida* showed higher proportions in 2015 and 2016 than in 2014 or 2017. *Reophax arctia* and *Reophax nana* increased in 2017 with reference to the years before (Fig. 7).

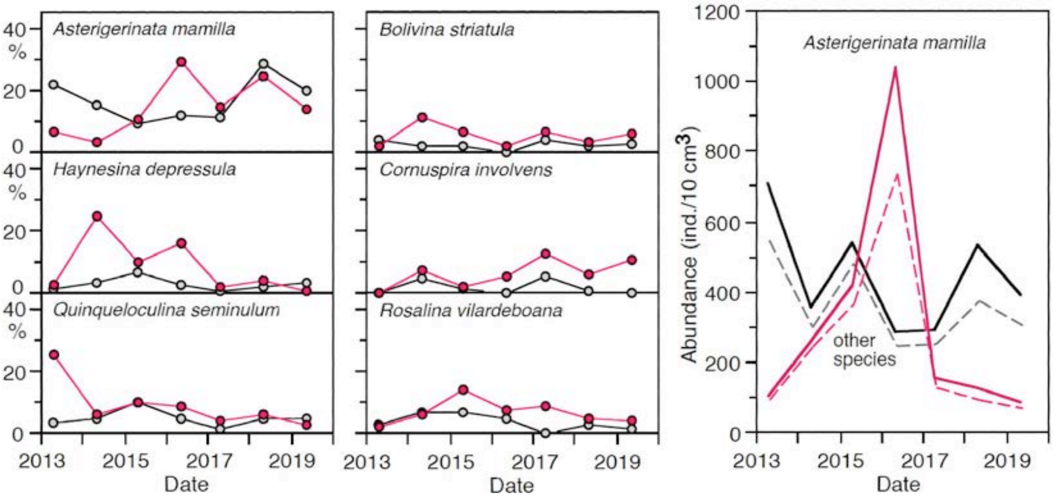

Fig. 8. Time series of the six-ranked species of the living (rose-Bengal stained) fauna from the 63-2000 µm grain size fraction of the 0-1 cm surface sediment at Esteiro do Ancão monitoring site, 30 m. Right panel: population densities of *Asterigerinata mamilla* (lines) and other species (dashed lines) during the investigation period. Pink dots and lines: living fauna, grey dots and lines: dead assemblage.

The benthic foraminiferal population densities showed a skewed bell-shaped pattern along the backbarrier beach transect with low values in the upper part, high values in the middle part, and intermediate values in the lower part and on the mud bank (Fig. 7). The maximum values ranged from 372 to 512 individuals 10 cm^{-3}. This pattern holds true for the distributions in 2014 and 2017. The population densities in the middle two years 2015 and 2016 rather depicted a staircase pattern with low values in the upper part and an abrupt rise to high values at around 20 m. The maximum values were in the range of 527 to 1084 individuals 10 cm^{-3}.

The 30-m time series station showed a similar pattern (Fig. 8, Supplement Table 9). *Asterigerinata mamilla* increased in abundance in 2015, showed a maximum in 2016 and slightly decreased again. The proportions of *Haynesina depressula* and *Quinqueloculina seminulum* concomitantly decreased while the other species showed only minor variations. The population densities were on the rise since 2013, showed a maximum in 2016, and declined again from 2017 onwards. The peak in 2016 was further amplified by the high absolute abundance of *A. mamilla*.

3.4 Dead foraminiferal assemblages

At the 30-m time series station, 61 different foraminiferal species were found in the dead assemblages, of which 10 were not recorded in the living fauna (Appendix 1, Supplement Table 9). The majority of 37 species were rotaliids, 15 species were miliolids, and 9 species were textulariids. The most abundant species were *Asterigerinata mamilla, Cibicides lobatulus, Quinqueloculina laevigata, Ammonia tepida, Quinqueloculina seminulum* and *Elphidium gerthi.* They comprise between 47 and 60 % of the dead assemblage, and their individual proportions range from 1.5 to 28.2 %, on average 9.0 %. The other species range from 0.4 to 7.5 % only. The dead assemblages include a substantial portion of robust, near-shore shelf foraminifera, for instance *Eponides repandus*, Elphidium advenum, Quinqueloculina agglutinata and *Cibicides lobatulus*, the latter in high numbers. Their tests are very large, yellow-stained, worn and polished. In *Cibicides lobatulus*, intergrade forms to the usual small and translucent specimens of the dead assemblage were recognised.

The Fisher alpha diversity indices of the dead assemblages ranged from 8.8 to 15.1 and showed a slightly lower variability than in the corresponding living faunas (Fig. 6b). In both assemblages, the Fisher alpha index values were markedly lower in 2016 than in samples from the other years. The absolute abundances of dead foraminifera showed an irregular variability and did not follow the trend of the living fauna (Fig. 8). With the exception of 2016, the abundances of dead foraminifera were on average higher by a factor of 2.5 than the population densities of the living fauna. This ratio is of the same magnitude as figures from intertidal sands at São Vincente, Cape Verdes (5.3; Schönfeld and Lübbers, 2020), though substantially lower than in muddy sands on the outer Gulf of Cadiz shelf (24.7; Schönfeld, 2002).

The proportions of the six-ranked species of the living fauna were often slightly lower in the dead assemblages. *Cornuspira involvens*, *Bolivina striatula* and *Quinqueloculina seminulum* showed very similar variations as in the living fauna, whereas *Haynesina depressula* and *Rosalina vilardeboana* roughly follow their trend at the 30-m time series station. *Asterigerinata mamilla* showed non-congruent fluctuations as compared to their proportions in the living fauna, in particular a marked rise in percentages from 2017 to 2018 (Fig. 8).

4 Discussion

4.1 Hydrographical impact of inlet relocation

Ria Formosa is considered as multiple-inlet lagoon system with a complex hydrodynamics (Fabião et al., 2016; Pacheco et al., 2008, 2010; Salles et al., 2005). The inlets, their sedimentary dynamics, water transport and exchange with adjacent coastal sea have received much attention (Cravo and Jacob, 2019; Morris et al., 2001; Rosa et al., 2019; Vila-Concejo et al., 2004). Literature data suggested that the Ancão inlet lost hydraulic efficiency during the south-eastward migration in the 2000s and the tidal prism decreased (Jacob and Cravo, 2019; Vila-Concejo et al., 2003), while other studies considered the influence on its hydrodynamic behaviour and tidal prism as rather low (Pacheco et al., 2007). Our new data suggested that Ancão inlet relocation in 2015 indeed has effected the hydraulic parameters in distal parts of Ria Formosa lagoon. The Mean Tidal Level and difference between predicted and measured High Tide levels increased by 0.12 m and 0.2 m respectively, and the mean flood period extended by 0:07 h while the mean ebb period shortened. The average time lag between observation and prediction shortened by 0:21 h for High Tides and by 0:27 h for Low Tides. The total volume changes of the tidal prism could not be estimated but it is clear from the above figures that the flood gained more influence and a much better connectivity to the adjacent coastal sea that was achieved by the inlet relocation.

The obvious consequence of higher High Tide levels and shorter ebb tides is a stronger hydraulic gradient and more vigorous ebb currents in the Esteiro do Ancão. The average current velocity during a flood or ebb period depends on the tidal amplitude. As the Low Tide levels did not change with inlet relocation, the increase in tidal amplitude is effected by the rise in High Tide levels, i.e. 0.2 m. The relationships of mean current velocities and tidal amplitude suggested velocities higher by 0.04 m s^{-1} for ebb periods and by 0.03 m s^{-1} for flood periods at 0.2 m higher tidal amplitudes. Such an increase in flow strength by a few centimetres per second appears to be minute. None-the-less, pervasive erosional features were recognised at the beach backbarrier transect.

At other two inlets of Ria Formosa system, Faro-Olhão and Armona inlets, the tidal curves were sinusoidal and hence in good agreement with the astronomical model (Jacob et al., 2013; Fabião et al., 2016; Rosa et al., 2019). The tidal curve taken at Ponte da Praia de Faro shows a triangular shape rather than a sinus function. Triangular curves are typical for estuaries, in particular if they were assessed at distance to the mouth of the estuary (Boehlich, 2003; Gönnert et al., 2004).

It has to be emphasised that the effect of conduits under the dam to Praia de Faro are not captured by our measurements. It is also clear that the effects for the overall intertidal area to the Northwest of the dam are with ca. 2 % more submergence time rather small. Therefore, faunal and floral changes or displacements of the salt marshes and tidal flats are expected to be less severe.

4.2 Sedimentary and macrofaunal responses

Erosion after inlet relocation was particularly recorded at the beginning of the investigated transect. The brink at the spring high water line was set back, which caused a reduction of space for dry lawn and dune vegetation. To the Northwest of the transect, more than 20 cm of sand was missing at the foot of brick walls of the holiday estates. Backbarrier beaches at Ria Formosa were considered as rather stable (Carrasco and Matias, 2019). They rely on the input of wind-blown sand and overwash, which is not available in the urbanised area of Praia de Faro (Fig. 2). It is yet unclear whether the erosion in the upper part was effected by coincidence of spring high water and strong, storm-generated wave energy (e.g. Carrasco et al., 2012), or whether the loose, medium sand was more easily erodible at higher spring high waters and stronger currents than coarse sand with pebbles at lower levels in the transect. Further, down in section, however, the disappearance of the saltmarsh peat, reduction of water level marks and megaripples, and the incision of the runnel before the mud bank were recognised. All these observations indicate that extensive erosion was taking place after inlet relocation. A net loss of sediment was recorded in the upper part up to 7 m, and in the lower part of the slope between 30 and 35 m. It is noteworthy that the respective level of -0.7 to -0.9 m POD well corresponds to the interval of -0.5 to -1 m POD where the strongest tidal currents were recorded under Ponte da Praia de Faro (Fig. 5).

A gain in sediment was recorded on the mud bank that silted up by 0.18 m since the inlet relocation. The bank also prograded landwards by 4 m. A higher sand content was recognised in foraminiferal sample residues from the mud bank after 2015, even though it could not be quantified because the samples were analysed in a wet stage. It is conceivable that accumulation and mud bank accretion was promoted by sediment baffling of the dense *Zostera* vegetation on the bank (Potouroglou et al., 2017). None-the-less, the sediment accumulation after inlet relocation is about double as high as reported in the literature (Carrasco and Matias, 2019).

While the changes in sedimentary environment were recognised from one year to the other, the macrofaunal changes took place more slowly. A distinctive pattern discriminating the situation before and after inlet relocation was blurred by the high inter-annual variability of macrofaunal abundance as recorded by sediment surface inspection. The only pervasive change was the diminishing and erosion of firmgrounds and the establishment of polychaeta colonies. Firmgrounds are agglomerations of sessile, encrusting organisms which develop on poorly consolidated sands or pebbles (e.g. Freitas et al., 1994). Such agglomerations may be broken up easily, for instance by wave action in shallow waters, the fragments were abraded and redeposited. They were shaped to nodules, which again providing substrates for other calcifiers (Baarli et al., 2012, and references therein). At Esteiro do Ancão however, the firmground patches successively diminished, hence were probably fragmented at their edges, although erratic clasts or firmground-derived nodules were not found. Among the attached organisms, the small oysters disappeared while the large *Ulva* sustained as it also used large pebbles to anchor (Aníbal, 2019).

The recruitment and growth of polychaet colonies took a couple of years. They replaced the firmground biocoenosis. Tube-building polychaets may form dense aggregations, which are patchy distributed and even may reach sizes of up to 15 m^2 (Degraer et al., 2008). The colonies thrive under specific hydrodynamic settings with varying currents (Van Lancker et al., 2013). They prefer comparatively fine sands at shallow depths to build their colonies (Van Hoey et al., 2008), which was also recognised at Esteiro do Ancão. A variety of species are involved (e.g. *Lanice conchilega, Owenia fusiformis, Sabellaria alveolata*), and they have a high filtering efficiency (Dubios et al., 2003). It is therefore conceivable that polychaete colonies effectively remove food particles from the near-bottom flow in Esteiro do Ancão.

4.3 Benthic foraminiferal response pattern

The foraminiferal response to environmental changes after inlet relocation was faster and more profound than with sessile macrofauna. The population densities almost doubled and the faunal composition shifted to high proportions of *Asterigerinata mamilla* from 2015 to 2016. While higher proportions of this species remained, the faunal population density decreased in 2017 to values as before. A precursor of this dynamics was recognised in spring 2015 already, when population densities along the transect changed from a bell-shaped to a staircase pattern, though dredging the new inlet has not commenced. However, extensive construction works in the entire area took place in spring 2015, with intensive traffic of caterpillars and trucks in the intertidal area of the northwestern part of Ria Formosa. It is plausible that these activities extensively disturbed the sediment and facilitated an enhanced release of nutrients from subsurface sediment layers (e.g. Asmus et al., 2000; Falcao and Vale, 1990). The nutrients released may have promoted at first microphytobenthos growth, which lives in the first millimetres of the sediment and is an important food source for benthic foraminifera (Aníbal, 2019; Austin et al., 2005; Brito et al., 2009; Domingues et al., 2017; Papaspyrou et al., 2013). Despite these benthic-pelagic exchange processes, primary production and algal growth may also be fuelled by upwelling-originated, nutrient-rich shelf waters transported into the lagoon by tidal inflow, or by nitrate-rich groundwater discharges (e.g. Cravo and Jacob, 2019; Falcão and Vale, 1990; Leote et al., 2008; Loureiro et al., 2006; Newton and Mudge, 2005). Nutrient or chlorophyll data from spring 2015 measured on Ria Formosa and adjacent Gulf of

Cadiz waters were not available to constrain the influence of the latter sources and processes. In any case, a higher flux of food particles, let it be vertical or lateral by near-bottom currents, is known to be mirrored by higher benthic foraminiferal population densities (Altenbach, 1992; Morigi et al., 2001; Schönfeld and Numberger, 2007).

The situation amplified when the new inlet has been built and extensive erosion probably effected a further release of nutrients from subsurface sediments. Unfortunately, nutrient measurements were not performed in the Esteiro do Ancão before inlet relocation, neither concentrations of chlorophyll or suspended particles were assessed in the near-bottom water on-site and before our foraminiferal sampling. However, a few qualitative observations corroborated the above presumption. The salt marsh plants on the opposite side of Esteiro do Ancão were stronger and greener in 2016 than during the sampling campaigns in the previous years. The spring temperatures were even lower in 2015 than in the year before in that the good plant state is considered a matter of enhanced nitrate or phosphate availability. Nutrient measurements on water samples taken in April and May revealed a general decline of average nitrate concentrations in ebb waters from 2017 to 2019 (Supplement Table 10). Nitrate and phosphate concentrations in 2018 were in good agreement with data from spring 2012 (Cravo and Jacob, 2019). It has to be noted that nutrient concentration in Ria Formosa waters showed strong seasonal and interannual variations (e.g. Barbosa, 2010). Therefore, our punctual measurements have to be considered with caution, even though sampling and analyses have been done systematically and with great care.

Erosion was recognised on the investigated backbarrier transect, but certainly also has been the case in smaller, tributary affluents of Esteiro do Ancão further upstream. Accommodation and stabilisation of the sedimentary systems may well have reduced the nutrient release and growth of microphytobenthos during the last years while new filter-feeding communities established. It is conceivable that food particle availability declined and consequently the foraminiferal population densities fall back to levels before inlet relocation. Non-the-less, *Asterigerinata mamilla* sustained with high proportions of the fauna. This species is known to prevail on sandy substrate (Barras et al., 2014; Dimiza et al., 2016; Pujos, 1976) in turbulent, clear waters (Wilson and Hayek, 2019) at shallow water depths (Mendes et al., 2004; Milker and Schmiedl, 2012), and may even pursue an epiphytic lifestyle (Frezza et al., 2010). It has also been recorded in the outer Guadiana estuary where it only was found during winter (Camacho et al., 2015), though it has not been recorded in the inner Bay of Cádiz (Papaspyrou et al., 2013: their Supplement Table S1). In our study, *A. mamilla* has been observed attached to large sand grains in samples from the investigated transect at Esteiro do Ancão. Therefore, this species is considered to be more resilient to substrate instability than other benthic foraminifera, thus has a competition advantage, which again is mirrored in higher proportions of this species.

Asterigerinata mamilla is also the most frequent species in the dead assemblages an the 30-m monitoring site. Their proportions even exceed those of the living fauna in four of seven samples. The composition of the living fauna and dead assemblage in surface sediments from the same site is often largely different (e.g. Murray, 1976). Biotic processes, as the differential delivery of empty tests to the sediment by individual species (e.g. Jorissen and Wittling, 1999), post-mortem processes as corrosion, redeposition and bioturbational mixing (e.g. Murray and Pudsey, 2004; Wang and Chappell, 2001), and diagenetic effects (e.g. Walker and Goldstein, 1999) account for the difference between the living fauna and dead assemblage. The abundances of common species in the dead assemblages non-the-less follow their trend in the living faunas at the 30-m monitoring site (Fig. 8). Furthermore, the diversity of the dead assemblage was as low as in the living fauna in 2016. These patterns indicate an instant delivery of empty tests from the living fauna to the dead assemblage at comparable rates among species (e.g. Mendes et al., 2013). The attenuation of their fluctuations in the dead assemblages revealed, on the other hand, that also a constant loss of tests prevailed in this current-swept environment. The net erosion by 0.1 m at the monitoring site from 2013 to 2019 (Fig. 3), and the considerable enrichment of yellow-stained and worn tests of near-shore foraminiferal species, corroborate the contention that omission rather than accumulation prevailed at the monitoring site. Non-the-less, the proportion and abundance of *Asterigerinata mamilla* increased in the dead assemblage in 2018, two years after the bloom of this species in the living fauna. Microhabitat preference and competition advantage of this species, as discussed above, may have led to a higher test production. The lag of two years probably mirrors the time that was necessary to facilitate a sufficient accumulation of empty tests in the surface sediment. The lag might also be effected by an extended life cycle of ca. 1.5 to 2 years. This appears to be less likely because a long-living species could not respond so rapidly to the changing environmental conditions as in 2016. Furthermore, experimental evidences suggest a rapid maturation and growth of *Asterigerinata mamilla* during six weeks (Weinmann et al., 2019). The enrichment of empty tests in the dead assemblage might also be the product of a mass mortality before sampling in 2018. With the given low population density in 2017, a single-event production of a 3.5-fold higher number of tests (Supplement Table 9), to be accumulated and sustaining in this current-swept environment, appears to be less likely as well.

4.4 Implications for foraminiferal monitoring

The results of the present study showed that inlet relocation and anthropogenic activities in the northwestern Ria Formosa had two interfering effects. First, nutrient release by near-surface sediment disturbance and erosion may have fuelled an enhanced microphytobenthos growth in 2015 and 2016, which is depicted in higher benthic foraminiferal population densities and higher proportions of *Ammonia tepida* (e.g. Papaspyrou et al., 2013; Haynert et al., 2020). This short-term bloom is not recorded in the dead foraminiferal assemblages despite of their lower diversity in 2016. Second, the inlet relocation induced tidal current invigoration, which is instantaneously mirrored by higher abundances of *Asterigerinata mamilla*. Faunal change is recorded in the dead assemblages with a certain delay. Therefore, the dead assemblages are deemed not being suitable for environmental monitoring (Duros et al., 2012; Schönfeld et al., 2012).

Our data indicated that when a limiting environmental variable exceeds a certain threshold, the faunal composition and population density changed to a new state. However, the faunal composition, diversity and density fall back, once the respective variable returns to the conditions that prevailed before. Therefore, the initial hypothesis of the present study is rejected.

The present study also demonstrated that foraminifera responded much faster to environmental perturbations than macroorganisms. In contrast to these findings and despite all attempts of the FOBIMO initiative (Alve et al., 2016; Schönfeld et al., 2012), the official guidelines only consider the macrofauna for biomonitoring and ecosystem status assessments in most European countries.

5 Conclusions

The foraminiferal communities responded immediately to the tidal current acceleration in the Esteiro do Ancão after inlet relocation, nutrient release and enhanced microphytobenthos growth. Even though we have only indirect evidences for the latter due to the lack of primary productivity data, chlorophyll or nutrient measurements from spring 2015, the foraminiferal faunas clearly showed a response by a rise in population densities, intensified by a bloom of a single species. A marked, promoting factor was the resilience of *Asterigerinata mamilla* to substrate instability as revealed by the present study. Antagonistic effects were the subsequent change in macrofauna to polychaeta colonies with a high filtering efficiency. Food impoverishment has led to an abundance decline of *A. mamilla* and other species. The high proportions of *A. mamilla* in the living fauna sustained while the tidal currents remained at higher levels than before inlet relocation. This observation credences credibility to earlier data from the Gulf of Cadiz (Schönfeld, 2002), where a linear relationship of living epibenthic foraminiferal percentages and current velocities at intermediate depths was recognised.

The initial hypothesis of the present study is rejected. When a limiting environmental variable exceeds a certain threshold, the faunal composition and population density changed to a new state. The faunal composition, diversity and density immediately fall back, once the respective variable returns to the conditions that prevailed before. The record of the dead assemblages is less clear and delayed.

The mutual response again depicted living benthic foraminifera as powerful environmental indicators. They responded much faster to environmental perturbations than macroorganisms. None-the-less, official guidelines mainly consider macrofaunal data for ecosystem status assessments in most European countries.

Acknowledgements

The authors are indebted to Óscar Ferreira, Andre Pacheco and Margarida Ramirez, Universidade do Algarve, Faro, for rare literature, hight reference data, D-GPS measurements, logistical support and advice. Anke Dettner-Schönfeld is thanked for levelling assistance. Wolfgang Kuhnt gave access to the reference collection and Sebastian Beil maintained the photomicroscope facilities at the Micropaleontological Unit of the Institute of Geosciences, Kiel University. Regina Surberg, GEOMAR, Kiel, measured the nutrient concentrations in water samples from Ria Formosa. Patrons and staff of *Aeromar* and *MarSol*, Praia de Faro, are thanked for their hospitality during breaks of hydrocast deployments and after hours of sampling campaigns. Isabel Mendes thanks to Fundação para a Ciência e a Tecnologia for Research Assistant contract DL57/2016/CP1361/CT0009 and project UID/0350/2020 CIMA.

Author statement

IM and JS designed the study. JS and IM collected the samples and field data. JS analysed the results and drafted the manuscript. Both authors discussed the results and edited the manuscript. This work is part of the Strategic Research Program “OCEANS: From the deep-sea to the atmosphere“ financed by the Helmholtz Association, Germany.

Declaration of competing interests

The authors declare that they have no known competing financial interests or personal relationships that could have appeared to influence the work reported in this paper.

References

Alley, R.B., Meese, D.A., Shuman, C.A., Gow, A.J., Taylor, K.C., Grootes, P.M., White, J.W.C., Ram, M., Waddington, E.D., Mayewski, P.A., Zielinski, G.A., 1993. Aprupt increase in Greenland snow accumulation at the end of the Younger Dryas event. Nature 362, 527-529.

Altenbach, A.V., 1992. Short term processes and patterns in the foraminiferal response to organic flux rates. Marine Micropaleontology 19, 119-129.

Alve, E. and Bernhard, J.M., 1995. Vertical migratory response of benthic foraminifera to controlled oxygen concentrations in an experimental mesocosm. Marine Ecology Progress Series 116, 137-151.

Alve, E., Korsun, S., Schönfeld, J., Dijkstra, N., Golikova, E., Hess, S., Husum, K. and Panieri, G., 2016. Foram-AMBI: A sensitivity index based on benthic foraminiferal faunas from North-East Atlantic and Arctic fjords, continental shelves and slopes. Marine Micropaleontology 122, 1-12.

Aníbal, J., 2019. Ecological dynamics of green macroalgae Ulvales in Ria Formosa: a tale of blooms and shapes. In: Aníbal, J., Gomes, A., Mendes, I., Moura, D. (Eds.), Ria Formosa: challenges of a coastal lagoon in a changing environment. 1st edition, University of Algarve, Faro, pp. 83-98.

Andrade, C., Freitas, M.C., Moreno, J., Craveiro, S.C., 2004. Stratigraphical evidence of late Holocene barrier breaching and extreme storms in lagoonal sediments of Ria Formosa, Algarve, Portugal. Marine Geology 210, 339-362.

Asmus, R., Sprung, M., Asmus, H., 2000. Nutrient fluxes in intertidal communities of a South European lagoon (Ria Formosa) – similarities and differences with a northern Wadden Sea bay (Sylt-Rømø Bay). Hydrobiologia 436, 217-235.

Austin, H.A., Austin, W.E.N., Paterson, D.M., 2005, Extracellular cracking and content removal of the benthic diatom *Pleurosigma angulatum* (Quekett) by the benthic foraminifera *Haynesina germanica* (Ehrenberg). Marine Micropaleontology 57, 68-73.

Baarli, B.G., Santos, A., Da Silva, C.M., Ledesma-Vázquez, J., Mayoral, E., Cachão, M., Johnson, M.E., 2012. Diverse macroids and rhodoliths from the Upper Pleistocene of Baja California Sur, Mexico. Journal of Coastal Research 28, 296-305.

Banner, F.T., and Culver, S.J., 1978. Quaternary *Haynesina* n. gen. and Paleogene *Protelphidium* Haynes; their morphology, affinities and distribution. Journal of Foraminiferal Research 8, 177-207.

Barbosa, A.B., 2010. Seasonal and interannual variability of planktonic microbes in a mesotidal coastal lagoon (Ria Formosa, SE Portugal): impact of climatic changes and local human influences. In: Paerl, H. and Kennish, M. (Eds.), Coastal Lagoons: critical habitats of environmental change. CRC Press, Taylor & Francis Group, Marine Science Book Series, Boca Raton, pp. 335-366.

Barras, C., Jorissen, F.J., Labrune, C., Andral, B., Boissery, P., 2014. Live benthic foraminiferal faunas from the French Mediterranean Coast: towards a new biotic index of environmental quality. Ecological Indicators 36, 719-743.

Boehlich, M.J., 2003. Tiededynamik der Elbe. Mitteilungsblatt der Bundesanstalt für Wasserbau 86, 55-60.

Boltovskoy E., Wright R.,1976. Ecology. In: Boltovskoy E., Wright R. (Eds.), Recent Foraminifera Springer Netherlands, Dordrecht. pp. 223-274.

Bond, G., Broecker, W., Johnson, S., McManus, J., Labeyrie, L., Jouzel, J., Bonani, G., 1993. Correlations between climatic records from North Atlantic sediments und Greenland ice. Nature 365, 143-147.

Bouchet, V.M.P., Alve, E., Rygg, B., Telford, R.J., 2012. Benthic foraminifera provide a promising tool for ecological quality assessment of marine waters. Ecological Indicators 23, 66-75.

Brito, A., Newton, A., Tett, P., Fernandes, T.F., 2009. Temporal and spatial variability of microphytobenthos in a shallow lagoon: Ria Formosa (Portugal). Estuarine, Coastal Shelf Science 83, 67-76.

Brodniewicz, I.,1972. Pleistocene foraminifers of the area of the Lower Vistula River (northern Poland). Acta Palaeontologica Polonica 17, 423-525.

Camacho, S., Moura, D., Connor, S., Scott, D.B., Boski, T., 2015. Ecological zonation of benthic foraminifera in the lower Guadiana Estuary (southeastern Portugal). Marine Micropaleontology 114, 1-18.

Cantin, N.E., Cohen, A.L., Karnauskas, K.B., Tarrant, A.M., McCorkle, D.C., 2010. Ocean Warming Slows Coral Growth in the Central Red Sea. Science 329, 322-325.

Dansgaard, W., Johnson, J.J., Clausen, B.H., Dahl- Jensen, D.N.S., Gundestrup, N.S., Hammer, C.U., Hvidberg, C.S., Steffensen, J.P., Sveinbjörndottir, A.E., Jouzel, J., Bond, G., 1993. Evidence for general instability of past climate from a 250- kyr ice-core record. Nature 364, 218-220.

Carrasco, A.R., Ferreira, Ó., Matias, A., Freire, P., 2012. Natural and human-induced coastal dynamics at a back-barrier beach. Geomorphology 159-160, 30-36.

Carrasco, A.R., Matias, A., 2019. Backbarrier shores along the Ria Formosa lagoon. In: Aníbal, J., Gomes, A., Mendes, I., Moura, D. (Eds.), Ria Formosa: challenges of a coastal lagoon in a changing environment. 1st edition, University of Algarve, Faro, pp. 17-28.

Cravo, A., Jacob, J., 2019. Role of the Ria Formosa inlets on the physical, chemical and biological exchanges with the adjoining ocean. In: Aníbal, J., Gomes, A., Mendes, I., Moura, D. (Eds.), Ria Formosa: challenges of a coastal lagoon in a changing environment. 1st edition, University of Algarve, Faro, pp. 29-46.

Darling, K.F., Schweizer, M., Knudsen, K.L., Evans, K.M., Bird, C., Roberts, A., Filipsson, H.L., Kim, J.-H., Gudmundsson, G., Wade, C.M., Sayer, M.D.J., Austin, W.E.N., 2016. The genetic diversity, phylogeography and morphology of Elphidiidae (Foraminifera) in the Northeast Atlantic. Marine Micropaleontology 129, 1-23.

Degraer, S., Moerkerke, G., Rabaut, M., Van Hoey, G., Du Four, I., Vincx, M., Henriet, J.-P., Van Lancker, V., 2008. Very-high resolution side-scan sonar mapping of biogenic reefs of the tube-worm *Lanice conchilega*. Remote Sensing of Environment 112, 3323-3328.

Dias, J.M., Sousa, M., Bertin, X., Fortunato, A.B., Oliveira, A., 2009. Numerical modeling of the impact of the Ancão Inlet relocation (Ria Formosa, Portugal). Environmental Modelling Software 24, 711-725.

Dimiza, M.D., Triantaphyllou, M.V., Koukousioura, O., Hallock, P., Simboura, N., Karageorgis, A.P. and Papathanasiou, E., 2016. The Foram Stress Index: A new tool for environmental assessment of soft-bottom environments using benthic foraminifera. A case study from the Saronikos Gulf, Greece, Eastern Mediterranean. Ecological Indicators 60, 611-621.

Dolven, J.K., Alve, E., Rygg, B., Magnusson, J., 2013. Defining past ecological status and in situ reference conditions using benthic foraminifera: a case study from the Oslofjord, Norway. Ecological Indicators 29, 219-233.

Domingues, R.B., Guerra, C.C., Barbosa, A.B., Galvão, H.M., 2017. Will nutrient and light limitation prevent eutrophication in an anthropogenically-impacted coastal lagoon? Continental Shelf Research 141, 11-25.

Dubois, S., Barillé, L., Retière, C., 2003. Efficiency of particle retention and clearance rate in the polychaete *Sabellaria alveolata* L. Comptes Rendus Biologies 326, 413-421.

Duffield, C.J., Hess, S., Norling, K., Alve, E., 2015. The response of *Nonionella iridea* and other benthic foraminifera to “fresh” organic matter enrichment and physical disturbance. Marine Micropaleontology 120, 20-30.

Duros, P., Fontanier, C., de Stigter, H.C., Cesbron, F., Metzger, E., Jorissen, F.J., 2012. Live and dead benthic foraminiferal faunas from Whittard Canyon (NE Atlantic): focus on taphonomic processes and paleo-environmental applications. Marine Micropaleontology 94-95, 25-44.

Elderfield, H., Yu, J., Anand, P., Kiefer, T., Nyland, B., 2006. Calibrations for benthic foraminiferal Mg/Ca paleothermometry and the carbonate ion hypothesis. Earth and Planetary Science Letters 250, 633-649.

Ellis, B.F., Messina, A., 1940. Cataloque of foraminifera. Micropaleontology Press, New York. Available from: http://www. micropress.org

Fabião, J.P.F., Rodrigues, M.F.G., Fortunato, A.B., Jacob, J.M.Q.B., Cravo, A.M.F., 2016. Water exchanges between a multi-inlet lagoon and the ocean: the role of forcing mechanisms. Ocean Dynamics 66, 173-194.

Falcão, M., Vale, C., 1990. Study of the Ria Formosa ecosystem: benthic nutrient remineralization and total variability of nutrients in the water. Hydrobiologia 207, 137-146.

Freitas, M.C., Cachao, M., Cancela da Fonseca, L., Caroça, C., Galopim de Carvalho, A.M., 1994. Unusual co-occurrence of serpulids an Bryozoa in a lagoonal system (Albufeira coastal lagoon - Portugal). Gaia 8, 39-46.

Frezza, V., Pignatti, J.S., Matteucci, R., 2010. Benthic foraminiferal biofacies in temperate carbonate sediment in the western Pontine Archipelago (Tyrrhenian Sea, Italy). Journal of Foraminiferal Research 40, 313–326.

Galvão, H.M., Mendes, P.J., Caetano, S.M., Icely, J.D., Newton, A., 2019. Role of microbes in the Ria Formosa lagoon. In: Aníbal, J., Gomes, A., Mendes, I., Moura, D. (Eds.), Ria Formosa: challenges of a coastal lagoon in a changing environment. 1st edition, University of Algarve, Faro, pp. pp. 67-81.

Gönnert, G., Isert, K., Giese, H., Plüss, A., 2004. Charakterisierung der Tiedenkurve. Die Küste 68, 99-141.

Hammer, Ø., Harper, D.A.T., Ryan, P.D., 2001. PAST. Paleontological statistics software package for education and data analysis. Palaeontologia electronica 4, 9 pp.

Harvey, B.P., Al-Janabi, B., Broszeit, S., Cioffi, R., Kumar, A., Aranguren-Gassis, M., Bailey, A., Green, L., Gsottbauer, C.M., Hall, E.F., Lechler, M., Mancuso, F.P., Pereira, C.O., Ricevuto, E., Schram, J.B., Stapp, L.S., Stenberg, S., Santa Rosa, L.T., 2014. Evolution of marine organisms under Climate Change at different levels of biological organisation. Water 6, 3545-3574.

Havach, S.M., Chandler, G.T., Wilson-Finelli, A., Shaw, T.J., 2001. Experimental determination of trace element partition coefficients in cultured benthic foraminifera. Geochimica and Cosmochimica Acta 65, 1277-1283.

Haynert, K., Gluderer, F., Pollierer, M.M., Scheu, S., Wehrmann, A., 2020. Food spectrum and habitat-specific diets of benthic foraminifera from the Wadden Sea – a fatty acid biomarker approach. Frontiers in Marine Science 7, 510288.

Haynes, J.R., 1973. Cardigan Bay Recent foraminifera. Bulletin of the British Museum (Natural History) Zoology, Supplement 4, 1-245.

Horten, B.P.and Edwards, R.J., 2006. Quantifying Holocene sea-level change using intertidal foraminiera: lessons from the British Isles. Cushman Foundation for Foraminiferal Research, Special Publication 40, 1-97.

Hughes, T., Kerry, J., Álvarez-Noriega, M., Álvarez-Romero, J., Anderson, K., Baird, A., Babcock, R.C., Beger, M., Bellwood, D.R., Berkelmans, R., Bridge, T.C., Butler, I., Byrne, M., Cantin, N.E., Comeau, S., Connolly, S.R., Cumming, G.S., Dalton, S.J., Diaz-Pulido, G., Eakin, C.M., Figueira, W.F., Gilmour, J.P., Harrison, H.B., Heron, S.F., Hoey, A.S., Hobbs, J.-P.A., Hoogenboom, M.O., Kennedy, E.V., Kuo, C., Lough, J.M., Lowe, R.J., Liu, G., McCulloch, M.T., Malcolm, H.A., McWilliam, M.J., Pandolfi, J.M., Pears, R.J., Pratchett, M.S., Schoepf, V., Simpson, T., Skirving, W.J., Sommer, B., Torda, G., Wachenfeld, D.R., Willis, B.L., Wilson, S.K., 2017. Global warming and recurrent mass bleaching of corals. Nature 543, 373-377.

Jacob, J., Cravo, A., 2019. Recent evolution of the tidal prisms at the inlets of the western sector of the Ria Formosa, south coast of Portugal. Regional studies in Marine Science 31, 100767, 9 pp.

Jacob, J., Cardeira, S., Rodrigues, M., Bruneau, N., Azevedo, A., Fortunato, A.B., Rosa, M., Cravo, A., 2013. Experimental and numerical study of the hydrodynamics of the western sector of Ria Formosa. Journal of Coastal Research, Special Issue 65, 2011-2016.

Jorissen, F.J., Wittling, I., 1999. Ecological evidence from live-dead comparisons of benthic foraminiferal faunas off Cape Blanc (Northwest Africa). Palaeogeography, Palaeoclimatology, Palaeoecology 149, 151-170.

Kleypas, J.A., Buddemeier, R.W., Archer, D., Gattuso, J.P., Langdon, C., Opdyke, B.N., 1999. Geochemical consequences of increased atmospheric CO_2 on coral reefs, Science 284, 118-120.

Le Cadre, V., Debenay, J.P., 2006. Morphological and cytological responses of Ammonia (foraminifera) to copper contamination: Implication for the use of foraminifera as bioindicators of pollution. Environmental Pollution 143, 304-317.

Lenton, T.M., Held, H., Kriegler, E., Hall, J.W., Lucht, W., Rahmstorf, S., Schellnhuber, H.J., 2008. Tipping elements in the Earth’s climate system. Proceedings of the National Academy of Sciences 105, 1786-1793.

Lenton, T.M., Rockström, J., Gaffney, O., Rahmstorf, S., Richardson, K., Steffen, W., Schellnhuber, H.J., 2019. Climate tipping points — too risky to bet against. Nature 575, 592-595.

Leote, C., Ibánhez, J.S., Rocha, C., 2008. Submarine groundwater discharge as a nitrogen source to the Ria Formosa studied with seepage meters. Biogeochemistry 88, 185-194.

Loeblich, A.R.Jr. and Tappan, H., 1988. Foraminiferal genera and their classification. Van Nostrand Reinhold Company, New York, 970 pp.

Loureiro, S., Newton, A., Icely, J.D., 2006. Boundary conditions for the European Water Framework Directive in the Ria Formosa lagoon, Portugal (physico-chemical and phytoplankton quality elements). Estuarine Coastal Shelf Science 67, 382-398.

Lübbers, J., Schönfeld, J., 2018. Recent saltmarsh foraminiferal assemblages from Iceland. Estuarine, Coastal and Shelf Science 200, 380-394.

Lutze, G.-F., Altenbach, A.V., 1991. Technik und Signifikanz der Lebendfärbung benthischer Foraminiferen mit Bengalrot. Geologisches Jahrbuch, Reihe A 128, 251-265.

Lutze, G.-F., Sarnthein, M., Koopman, B., Pflaumann, U., Erlenkeuser, H., Thiede, J., 1979. Meteor cores 12309: late Pleistocene reference section for interpretation of the Neogene of Site 397. Initial Reports on the Deep Sea Drilling Project 47, 727-739.

Manabe, S., Stouffer, R.J., 1988. Two stable equilibria of a coupled ocean - atmosphere model. Journal of Climate 1, 841-868.

Manabe, S., Stouffer, R.J., 1997. Coupled ocean-atmosphere model response to freshwater input: comparison to Younger Dryas event. Paleoceanography 12, 321-336.

Mayle, F.E., Cwynar, L.C., 1995. Impact of the Younger Dryas cooling event upon lowland vegetation of Maritime Canada. Ecological Monographs 65, 129-154.

Mendes, I., Dias, A., Schönfeld, J., Ferreira, Ó., 2012. Distribution of living benthic foraminifera on the northern Gulf of Cadiz continental shelf. Journal of Foraminiferal Research 42, 18-38.

Mendes, I., Dias, J.A., Schönfeld, J., Ferreira, Ó., Rosa, F., Lobo, F.J., 2013. Living, dead and fossil benthic foraminifera on a river dominated shelf (northern Gulf of Cadiz) and their use for paleoenvironmental reconstruction. Continental Shelf Research 68, 91-111.

Mendes, I., Gonzalez, R., Dias, J.M.A., Lobo, F., Martins, V., 2004. Factors influencing recent benthic foraminifera distribution on the Guadiana shelf (Southwestern Iberia). Marine Micropaleontology 51, 171-192.

Mendes, I., Lobo, F.J., Hanebuth, T.J.J., López-Quirós, A., Schönfeld, J., Lebreiro, S., Reguera, M.I., Antón, L., Ferreira, Ó., 2020. Temporal variability of flooding events of Guadiana River (Iberian Peninsula) during the middle to late Holocene: Imprints in the shallow-marine sediment record. Palaeogeography, Palaeoclimatology, Palaeoecology 556, 109900, 16 pp.

Milker, Y., Schmiedl, G. 2012. A taxonomic guide to modern benthic shelf foraminifera of the western Mediterranean Sea. Palaeontologia Electronica, 5.2.16A, 134 pp.

Miller, D., Ota, Y., Sumaila, R., Cisneros-Montemayor, A., Cheung, W., 2017. Adaptation strategies to climate change in marine systems. Global Change Biology 24. 10.1111/gcb.13829.

Mojtahid, M., Jorissen, F., Lansard, B., Fontanier, C., Bombled, B., Rabouille, C., 2009. Spatial distribution of live benthic foraminifera in the Rhône prodelta: Faunal response to a continental–marine organic matter gradient. Marine Micropaleontology 70, 177-200.

Morris, B.D., Davidson, M.A., Huntley, D.A., 2001. Measurements of the response of a coastal inlet using video monitoring techniques. Marine Geology 175, 251–272.

Murray, J.W., 1976. Comparative Studies of Living and Dead Benthic Foraminiferal Distributions, in Hedley, R.H., Adams, C.G. (eds.), Foraminifera, 2, pp. 45-109.

Murray, J.W., Pudsey, C.J., 2004. Living (stained) and dead foraminifera from the newly ice-free Larsen Ice Shelf, Weddell Sea, Antarctica: ecology and taphonomy. Marine Micropaleontology 53 (1-2), 67-81.

Newton, A., Mudge, S., 2005. Lagoon-sea exchanges, nutrient dynamics and water quality management of the Ria Formosa (Portugal). Estuarine, Coastal and Shelf Science 62, 405-414.

Nilsson, T., 1983. The Pleistocene. Geology and Life in the Quaternary Ice Age. Reidel, Dordrechtl Boston/London, 651 pp.

Nordberg, K., Polovodova Asteman, I., Gallagher, T.M, Robijn, A., 2017. Recent oxygen depletion and benthic faunal change in shallow areas of Sannäs Fjord, Swedish west coast. Journal of Sea Research 127, 46-62.

Pacheco, A., Ferreira, Ó., Williams, J.J., Garel, E., Vila-Concejo, A., Dias, J.A., 2010. Hydrodynamics and equilibrium of a multiple-inlet system. Marine Geology 274, 32-42.

Pacheco, A., Vila-Concejo, A., Ferreira, Ó., Dias, J.A., 2008. Assessment of tidal inlet evolution and stability using sediment budget computations and hydraulic parameter analysis. Marine Geology 247, 104-127.

Pacheco, A., Vila-Concejo, A., Ferreira, Ó., Dias, J.M.A., 2007. Present hydrodynamics of Ancão Inlet, 10 years after its Relocation. Proceedings of the Coastal Sediments '07 Conference. New Orleans, May 2007, pp. 1557-1570.

Papaspyrou, S., Diz, P., García-Robledo, E., Corzo, A., Jimenez-Arias, J.L., 2013. Benthic foraminiferal community changes and their relationship to environmental dynamics in intertidal muddy sediments (Bay of Cádiz, SW Spain), Marine Ecology Progress Series 490, 121-135,

Paus, A., 1989. Late Weichselian vegetation, climate, and floral migration at Liastemmen, North Rogaland, south-western Norway. Journal of Quaternary Science 4, 223-242.

Polovodova Asteman, I., Nordberg, K., 2013. Foraminiferal fauna from a deep basin in Gullmar Fjord: The influence of seasonal hypoxia and North Atlantic Oscillation. Journal of Sea Research 79, 40-49.

Potouroglou, M., Bull, J.C., Krauss, K.W., Kennedy, H.A., Fusi, M., Daffonchio, D., Mangora, M.M., Githaiga, M.N., Diele, K., Huxham, M., 2017. Measuring the role of seagrasses in regulating sediment surface elevation. Scientific Reports 7, 11917.

Potter, D.C., 1978. A circulat towing tank for calibrating plankton-net flowmeters. Laboratory Reference No. 78-32, National Marine Fisheries Service, Northeast Fisheries Center, Woods Hole, Massachusetts, 14 pp.

Pujos, M., 1976. Écologie des foraminifères benthiques et des thecamoebiens de la Gironde et du plateau continental sud-Gascongne. Aplication à la connaissance du Quaternaire terminal de la région ouest-Gironde. Memoires de l'Institute de Geologie du Bassin D'Aquitaine 8, 1-314.

Rahmstorf, S., 1994. Rapid climate transitions in a coupled ocean-atmosphere model. Nature 372, 82-85.

Riebesell, U., Zondervan, I., Rost, B., Tortell, P.D., Richard, E.Z., Morel, F.M.M., 2000. Reduced calcification of marine plankton in response to increased atmospheric CO_2, Nature 407, 364-367.

Rosa, A., Cardeira, S., Pereira, C., Rosa, M., Madureira, M., Rita, F., Jacob, J., Cravo, A., 2019. Temporal variability of the mass exchanges between the main inlet of Ria Formosa lagoon (southwestern Iberia) and the Atlantic Ocean. Estuarine, Coastal and Shelf Science 228, 106349, 13 pp.

Roucoux, K.H., Shackleton, N.J., de Abreu, L., Schönfeld, J., Tzedakis, P.C., 2001. Combined marine proxy and pollen analyses reveal rapid Iberian vegetation response to North Atlantic millenial-scale climatic oscillations. Quaternary Research 56, 128-132.

Salles, P., Voulgaris, G., Aubrey, D., 2005. Contribution of nonlinear mechanisms in the persistence of multiple tidal inlet systems. Estuarine Coastal Shelf Science 65, 475-491.

Schönfeld, J., 2002. A new benthic foraminiferal proxy for near-botton current velocities in the Gulf of Cadiz, northeastern Atlantic Ocean. Deep-Sea Research I 49, 1853-1875.

Schönfeld, J., Numberger, L., 2007. The benthic foraminiferal response to the 2004 spring bloom in the western Baltic Sea. Marine Micropaleontology 65, 78-95.

Schönfeld, J., 2012. History and development of methods in Recent benthic foraminiferal studies. Journal of Micropalaeontology 31, 53-72.

Schönfeld, J., 2018. Monitoring benthic foraminiferal dynamics at Bottsand coastal lagoon (western Baltic Sea). Journal of Micropalaeontology 37, 383-393.

Schönfeld, J., Alve, E., Geslin, E., Jorissen, F., Korsun, S., Spezzaferri, S., 2012. The FOBIMO (FOraminiferal BIo-Monitoring) initiative e towards a standardised protocol for soft-bottom benthic foraminiferal monitoring studies. Marine Micropaleontology 94–95, 1-13.

Schönfeld, J., Golikova, E., Korsun, S., Spezzaferri, S., 2013. The Helgoland Experiment - assessing the influence of methodologies on Recent benthic foraminiferal assemblage composition. Journal of Micropalaeontology 32, 161-182.

Schönfeld, J., Lübbers, J., 2020. Checklist, assemblage composition, and biogeographic assessment of Recent benthic foraminifera (Protista, Rhizaria) from São Vincente, Cape Verdes. Zootaxa 4731, 151-192.

Schönfeld, J., Zahn, R., de Abreu, L., 2003. Surface and deep water response to rapid climate changes at the Western Iberian Margin. Global and Planetary Change 36, 237-264.

Solomon, S., Plattner, G.K., Knutti, R., Friedlingstein, P., 2009. Irreversible climate change due to carbon dioxide emissions. Proceedings of the National Academy of Sciences 106, 1704-1709.

Sprung, P., 1994. Macrobenthic secondary production in the intertidal zone of Ria Formosa - a lagoon in southern Portugal. Estuarine, Coastal and Shelf Science 38, 539-558.

Steffensen, J. P., Andersen, K. K., Bigler, M., Clausen, H. B., Dahl-Jensen, D., Fischer, H., Goto-Azuma, K., Hansson, M., Johnsen, S., Jouzel, J., Masson-Delmotte, V., Popp, T., Rasmussen, S.O., Röthlisberger, R., Ruth, U., Stauffer, B., Siggaard-Andersen, M.L., Svenbjörnsdottir, A.E., Svensson, A., White, J.W.C., 2008. High-Resolution Greenland Ice Core Data Show Abrupt Climate Change Happens in Few Years. Science 321, 680-684.

Taylor, K.C., Lamorey, G.W., Doyle, G.A., Alley, R.B., Grootes, P.M., Mayewski, P.A., White, J.W.C., Barlow, L.K., 1993. The ‘flickering switch’ of late Pleistocene climate change. Nature 361, 432-436.

Tett, P., Gilpin, L., Svendsen, H., Erlandsson, C. P., Larsson, U., Kratzer, S., Fouilland, E., Janzen, C., Lee, J.-Y., Grenz, C., Newton, A., Ferreira, J. G., Fernandes, T., Scory, S., 2003. Eutrophication and some European waters of restricted exchange. Continental Shelf Research 23, 1635-1671.

Van Hoey, G., Guilini, K., Rabaut, M., Vincx M. and Degraer, S., 2008. Ecological implications of the presence of the tube-building polychaete *Lanice conchilega* on soft-bottom benthic ecosystems. Marine Biology 154, 1009-1019.

Van Lancker, V., Houziaux, J.S., Baeye, M., Van den Eynde, D., Rabaut, M., Troost, K., Vermaas, T., van Dijk, T.A.G.P., 2013. Biogeomorphology in the field: bedforms and species, a mystic relationship. Proceedings Marine and River Dune Dynamics – MARID IV – 15 & 16 April 2013, Bruges, Belgium, pp. 277-283.

Vila-Concejo, A., Ferreira, Ó., Matias, A., Dias, J.M.A., 2003. The first two years of an inlet: sedimentary dynamics. Continental Shelf Research 23, 1425-1445.

Vila-Concejo, A., Ferreira, Ó., Morris, B., Matias, A., Dias, J.A., 2004. Lessons from inlet relocation: examples from Southern Portugal. Coastal Engineering 51, 967-990.

Vilanueva, P.G. and Canuado, I.S., 1999, Los Discorbaceos y los Rotaliaceos (Foraminiferida) del margen septentrional del Golfo de Cadiz. Revista Academia de Ciencias 54, 205-244.

Walker, S.E., Goldstein, S.T., 1999. Taphonomic tiering: experimental field taphonomy of molluscs and foraminifera above and below the sediment-water interface. Palaeogeography, Palaeoclimatology, Palaeoecology 149, 227-244.

Wang, P., Chappell, J., 2001. Foraminifera as Holocene environmental indicators in the South Alligator River, Northern Australia. Quaternary International 83-85, 47-62.

Wefer, G., 1976. Umwelt, Produktion und Sedimentation benthischer Foraminiferen in der westlichen Ostsee. Reports Sonderforschungsbereich 95 Wechselwirkung Meer - Meeresboden 14, 1-103.

Weinmann, A.E., Goldstein, S.T., Triantaphyllou, M.V., Langer, M.R., 2019. Effects of sampling site, season, and substrate on foraminiferal assemblages grown from propagule banks from lagoon sediments of Corfu Island (Greece, Ionian Sea). PLoS ONE 14(6), e0219015, 51 pp.

Wilson, B., Hayek, L.A.C., 2019. Benthic foraminifera and the polychaete *Sabellaria alveolata* (Linnaeus, 1767) on the intertidal rocky shore at Ceinewydd, Ceredigion, Wales, UK. Marine Micropaleontology 146, 51-58.

Wit, J.C., de Nooijer, L.J., Wolthers, M., Reichart, G.-J., 2013. A novel salinity proxy based on Na incorporation into foraminiferal calcite. Biogeosciences, 10, 6375-6387.

WoRMS Editorial Board, 2020. World Register of Marine Species. Available from: http://www.marinespecies.org

Zahn, R., Schönfeld, J., Kudrass, H.-R., Park, M.-H., Erlenkeuser, H., Grootes, P., 1997. Thermohaline instability in the North Atlantic during meltwater events: stable isotope and ice-rafted records from core SO75-26KL, Portuguese Margin. Paleoceanography 12, 696-710.

Appendix 1. Benthic foraminiferal reference list

Note: The genera and species are listed in alphabetical order. Their type references are given by Ellis and Messina (1940), WoRMS Editorial Board (2020), and Loeblich and Tappan (1988). They are not included in the reference list of this paper. Species marked with an asterisk were recorded in the dead assemblages only.

Adelosina laevigata d'Orbigny 1826, p. 304; d'Orbigny (1846), p. 302, pl. 20, figs. 22-24.

Adelosina longirostra (d'Orbigny) = *Quinqueloculina longirostra* d'Orbigny 1826, p. 303; d'Orbigny (1846), p. 291, pl. 18, figs. 25-27.

Ammoglobigerina globigeriniformis (Parker and Jones) = *Lituola nautiloidea* var. *globigeriniformis* Parker and Jones 1865, p. 407, pl. 15, figs. 46, 47, pl. 17, figs. 96-98.

Ammonia aberdoveyensis Haynes 1973, p. 184, fig. 38, nos. 1-7, pl. 18, fig. 15.

Ammonia beccarii (Linné) = *Nautilus beccarii* Linné 1758, p. 710, pl. 1, figs 1a-c.

Ammonia tepida (Cushman) = *Rotalia beccarii* var*. tepida* Cushman, 1926, p. 79, pl. 1.

Ammoscalaria runiana (Heron-Allen and Earland) = *Haplophragmium runianum* Heron-Allen and Earland, 1916, p. 224, pl. 40, figs. 15-18.

Ammotium salsum (Cushman and Bronnimann) = *Ammobaculites salsus* Cushman and Bronnimann, 1948, p. 16, pl. 3, figs. 7-9.

Asterigerinata mamilla (Williamson) = *Rotalina mamilla* Williamson, 1858, p. 54, pl. 4, figs. 109-111.

Aubignyna hamblensis Murray, Whittaker and Alve 2000, p. 64, pl. 2, figs. 1-16, Fig. 1,a-c, e. Note: the species has been confused with *Aubignyna perlucida* (Heron-Allen and Earland 1913) or *Aubignyna planidorsa* (Atkinson, 1969) which is a junior synonym. The specimens from Ria Formosa are clearly planoconvex and high trochospiral with backwards curved sutures on the spiral side.

Bolivina dilatata Reuss 1850, p. 381, pl. 48, figs. 15a-c.

Bolivina italica Cushman 1936, p. 56, pl. 8, fig. 6.

Bolivina ordinaria Phleger and Parker 1952, (new name for *Bolivina simplex* Phleger and Parker, 1951, p. 14, pl. 7, fig. 4-6).

Bolivina pacifica Cushman and McCulloch = *Bolivina acerosa* Cushman var. *pacifica* Cushman and McCulloch 1942, p. 185, pl. 21, figs. 1-3.

Bolivina pseudoplicata Heron-Allen and Earland 1930, p. 81, pl. 3, figs. 36-40.

Bolivina striatula Cushman 1922, p. 27, pl. 3, fig. 10.

Bolivina subaenariensis Cushman 1922, p. 46, pl. 7, fig. 6.

Bolivina tongi Cushman, 1929, p. 93, pl. 13, figs. 29 a, b.

Note: the test chamber walls are slightly opaque and rather thick as compared to other *Bolivina* species.

Bolivina variabilis (Williamson) = *Textularia variabilis* Williamson 1858, p. 76, pl. 6, figs. 162, 163.

Bulimina elegans d'Orbigny 1826, p. 270.

Bulimina marginata d'Orbigny 1826, p. 269, pl. 12, figs. 10-12.

Buliminella elegantissima (d'Orbigny) = *Bulimina elegantissima* d'Orbigny, 1839, p. 51, pl. 7, figs. 13-14.

**Cassidulina laevigata* d'Orbigny 1826, p. 282, pl. 15, figs. 4, 5.

Cassidulina minuta Cushman 1933b, p. 92, pl. 10, fig. 3.

Cibicides lobatulus (Walker and Jacob) = *Nautilus lobatulus* Walker and Jacob, 1798, p. 642, pl. 14, fig. 36.

Cornuspira involvens (Reuss) = *Operculina involvens* Reuss, 1850, p. 370, pl. 46, fig. 20.

Crithionina granum Goës 1894, p. 15, pl. 3, figs. 28-33.

Crithionina mamilla Goës, 1894, p. 15, pl. 3, figs. 34-36.

Crithionina pisum Goës 1896, p. 24, pl. 2, figs. 1-2.

Deuterammina balkwilli Brönnimann and Whittaker 1983, p. 352, fig. 13-16, 26.

Deuterammina eddystonensis Brönnimann and Whittaker 1990, p. 118, pl. 4, figs. 1-8, pl. 8, fig. 2, pl. 4, figs. 1-4.

Deuterammina rotaliformis (Heron-Allen and Earland) = *Trochammina rotaliformis* Heron-Allen and Earland, 1911, p. 309. Referred to: *Trochammina inflata* (Montagu) var. Balkwill and Wright, 1885, p. 331, pl. 13, figs. 11-12.

Discorinopsis aguayoi (Bermúdez) = *Discorbis aguayoi* Bermúdez, 1935, p. 204, pl. 15, figs 10-14.

Eggerella europea (Christiansen) = *Verneuilina europeum* Christiansen, 1958, p. 66. (new name for *Verneuilina advena* Cushman emend. Höglund, 1947, pl. 13, figs. 11a-c, text fig. 169.)

Eggerelloides scaber (Williamson) = *Bulimina scabra* Williamson 1858: p. 65, pl. 5, figs. 136-137.

Elphidium advenum (Cushman) = *Polystomella advena* Cushman 1922, p. 56, pl. 9, figs. 11-12.

Elphidium complanatum (d'Orbigny) = *Polystomella complanata* d'Orbigny 1839, p. 129, pl. 2, figs. 35, 36.

Elphidium crispum (Linné) = *Nautilus crispus* Linnaeus 1758, p. 709.

Elphidium cuvillieri Levy 1966, p. 5, pl. 1, fig. 6, pl. 2. Note: This species has been considered to fall in the morphological variability of *Elphidium poeyanum* (d'Orbigny) by Brodniewicz (1972), and as a junior synonym of *Elphidium excavatum* (Terquem) by Horton and Edwards (2006). It was clearly destinguishable from the latter by Haynes (1973). In the Gulf of Cadiz, *Elphidium cuvillieri* was reported from outside the debouchement of Cadiz lagoon and shallow shelf around 30 m water depth (Villanueva and Canudo, 1999; Mendes et al., 2012).

Elphidium excavatum (Terquem 1875) = *Polystomella excavata* Terquem, p. 20, pl. 2, figs. 2a, b.

Elphidium gerthi van Voorthuysen 1957, p. 32, pl. 23, figs. 12a, b.

**Elphidium oceanensis* (d’Orbigny) = *Polystomella oceanensis* d'Orbigny 1826, p. 285, no. 8. Note: the illustration was provided by Fornasini (1904), p. 13, pl. 3, fig. 10.

**Elphidium poeyanum* (d’Orbigny) = *Polystomella poeyana* d’Orbigny 1839, p. 55, pl. 6, figs. 25, 26. Note: *Cribroelphidium poeyanum* of authors.

Elphidium williamsoni Haynes 1973, p. 207, pl. 24, fig. 7, pl. 25, figs. 6, 9, pl. 27, figs. 1-3.

Epistominella vitrea Parker 1953, p. 9, pl. 4, figs. 34-36, 40, 41.

**Eponides repandus* (Fichtel and Moll) = *Nautilus repandus* Fichtel and Moll 1798, p. 35, pl. 3, figs. a-d.

Fissurina lucida (Williamson) = *Entosolenia marginata* var. *lucida* Williamson, 1848, p. 17, pl. 2, fig 17.

**Gavelinopsis praegeri* (Heron-Allen and Earland) = *Discorbina praegeri* Heron-Allen and Earland 1913, p. 122, pl. 10, figs. 8-10.

Glabratella wrightii (Brady) = *Discorbina wrightii* Brady 1881, p. 413, pl. 21, fig. 6.

Glomospira gordialis (Jones and Parker) = *Trochammina squamata* (Jones and Parker) var. *gordialis* Jones and Parker, 1860, p. 304.

Guttulina communis (d'Orbigny) = *Polymorphina (Guttuline) communis* d'Orbigny 1826, p. 266, pl. 12, figs. 1-4.

Haynesina depressula (Walker and Jacob 1798) = *Nautilus depressulus* Walker and Jacob, p. 641, pl. 14, fig. 33. Note: The species has been assigned to the genus *Haynesina* by Banner and Culver (1978). Genetic data group *H. depressula* to a distinctively different clade than *Haynesina germanica* (Darling et al. 2016, fig. 2), hence the genus *Haynesina* may be polyphyletic.

Haynesina germanica (Ehrenberg) = *Nonionina germanica* Ehrenberg 1840: p. 23, pl. 2, figs. 1a–g.

Hopkinsina pacifica Cushman 1933, p. 86, pl. 8, fig. 16.

Jadammina macrescens (Brady) = *Trochammina inflata* (Montagu) var. *macrescens* Brady 1870: p. 290, pl. 11, figs. 5a–c.

Labrospira jeffreysii (Williamson) = *Nonionina jeffreysii* Williamson 1858, p. 34, pl. 3, figs. 72, 73. Note: *Cribrostomoides jeffreysii* of authors.

Lamarckina haliotidea (Heron-Allen and Earland) = *Pulvinulina haliotidea* Heron-Allen and Earland 1911, p. 338, pl. 11, figs. 6-11.

Lenticulina atlantica (Barker) = *Robulus atlanticus* Barker 1960, p. 144, pl. 69, figs. 10-12. Note: new name for *Cristellaria lucida* Thalmannn 1937.

**Lenticulina rotulata* (Lamarck) = *Lenticulites rotulata* Lamarck 1804, p. 188. Note: the type figure was given by Lamarck (1806), pl. 62, fig. 11.

Lepidodeuterammina eddystonensis (Brönnimann and Whittaker) = *Deuterammina (Lepidodeuterammina) eddystonensis* Brönnimann and Whittaker 1990, p. 118, pl. 8, fig. 2.

Lepidodeuterammina ochracea (Williamson) = *Rotalina ochracea* Williamson, 1858, p. 55, pl. 4, fig. 112, pl. 5, fig. 113.

Leptohalysis scotti (Chaster 1892) = *Reophax scottii* Chaster, p. 57, pl. 1, fig. 1.

**Massilina gualtieriana* (d'Orbigny) = *Quinqueloculina gualtieriana* d'Orbigny 1839, p. 186, pl. 11, figs. 1-3.

Miliammina fusca (Brady) = *Quinqueloculina fusca* Brady 1870: p. 286, pl. 11, fig. 2a-c.

Miliolinella circularis (Bornemann) = *Triloculina circularis* Bornemann 1855, p. 349, pl. 19, fig. 4.

Miliolinella hauerinoides (Rhumbler) = *Quinqueloculina subrotunda* f. *hauerinoides* Rhumbler 1936, p. 206, figs. 167, 208-121.

Miliolinella hybrida (Terquem) = *Quinqueloculina hybrida* Terquem 1878, p. 79, pl. 9, figs. 23a-c.

Mississippina concentrica (Parker and Jones) = *Pulvinulina concentrica* Parker and Jones 1864, p. 470, pl. 48, figs. 14a, b.

Morulaeplecta bulbosa Höglund 1947, p. 165, figs. 142a, b, pl. 12, figs. 2a, b.

Neoconorbina terquemi (Rzehak) = *Discorbina terquemi* Rzehak, 1888, p. 228. Note: new name for *Rosalina orbicularis* Terquem 1876.

Nonion fabum (Fichtel and Moll) = *Nautilus faba* Fichtel and Moll 1798, p. 103, pl. 19, figs. a-c.

Nonionella bradyi (Chapman) = *Nonionina scapha* (Fichtel and Moll) var. *bradii* Chapman, 1916, p. 71, pl. 5, fig. 42.

Nonionella iridea Heron-Allen and Earland 1932, p. 438, pl. 16, figs. 14-16.

Nonionoides grateloupii (d'Orbigny) = *Nonionina grateloupii* d'Orbigny 1839, p. 46, pl. 6, figs. 6-7.

Patellina corrugata Williamson 1858, p. 46, pl. 3, figs. 86-89.

Planorbulina mediterranensis d'Orbigny 1826, p. 280, pl. 14, figs. 4-6.

Portatrochammina haynesi (Atkinson) = *Trochammina haynesi* Atkinson 1969, p. 528, fig. 6, no. 1a-c.

Portatrochammina murrayi Brönnimann and Zaninetti 1984, p. 72, pl. 5, figs. 7, 12-15.

**Quinqueloculina agglutinata* Cushman 1917, p. 43, pl. 9, fig. 2.

**Quinqueloculina berthelotiana* d'Orbigny 1839, p. 142, pl. 3, figs. 25-27.

Quinqueloculina bicornis (Walker and Jacob) = *Serpula bicornis* Walker and Jacob 1798, p. 633, pl. 14, fig. 2.

Quinqueloculina bosciana d'Orbigny 1839, p. 191, pl. 11, figs. 22–24.

Quinqueloculina laevigata d'Orbigny 1826, p. 143, pl. 3, figs. 31–33.

Quinqueloculina lata Terquem 1876, p. 82, pl. 11, fig. 8.

Quinqueloculina limbata Fornasini 1905, p. 66, pl. 3, fig. 9.

Quinqueloculina parvula Schlumberger 1894, p. 255, pl. 3, figs. 8-9, text fig. 1.

Quinqueloculina rugosa d'Orbigny 1826, p. 302, no. 24. Note: *Cycloforina rugosa* (d'Orbigny) of authors.

Quinqueloculina seminulum (Linné 1758) = *Serpula seminulum* Linné, p. 786.

Quinqueloculina stelligera Schlumberger 1893, p. 68, pl. 2, figs. 58, 59, text fig. 17.

Rectuvigerina phlegeri Le Calvez 1959, p. 363, pl. 1, fig. 11; Mendes (2012). p. 38, fig. 3, nos. 7a, b.

Remaneica helgolandica Rhumbler 1938, p. 195, figs. 38-45.

Remaneica plicata (Terquem) = *Patellina plicata* Terquem 1876, p. 72, pl. 8, figs. 9a, b.

Reophax arctica Brady 1881, p. 405, pl. 21, fig. 2. Note: *Cuneata arctica* (Brady 1881) of authors.

Reophax moniliformis Siddall 1886, p. 54, pl. 1, fig. 2. Note: very similar but branched morphotypes were assigned to *Polysaccammina hyperhalina* Medioli, Scott, and Petrucci 1983 or *Protoschista findens* Parker 1870.

Reophax nana Rhumbler 1911, p. 182, pl- 8, figs. 6-12.

Rosalina bradyi (Cushman) = *Discorbis globularis* (d'Orbigny) var. *bradyi* Cushman, 1915, p. 12, pl. 8, fig. 1.

Rosalina cf. neapolitana (Hofker) = *Neoconorbina neapolitana* Hofker 1951, p. 438, figs. 300a-c, 301a-c.

Rosalina globularis d'Orbigny 1826, p. 271, pl. 13, figs. 1-4.

Rosalina macropora (Hofker) = *Discopulvinulina macropora* Hofker 1951, 460, figs. 312, 313.

Rosalina vilardeboana d'Orbigny 1839, p. 44, pl. 6, figs. 13-15.

Saccammina sphaerica Sars 1872, p. 250. Carpenter (1875), p. 532, fig. 272.

Siphonaperta quadrata (Nørvang) = *Quinqueloculina quadrata* Nørvang 1945, p. 7, pl. 1, fig. 2.

Spirillina vivipara Ehrenberg 1843, p. 323, pl. 3, fig. 41.

Spirorbina Sellier de Civrieux 1977, p. 35.

Stainforthia fusiformis (Williamson) = *Bulimina pupoides* var. *fusiformis* n. – Williamson1858, p. 63, pl. 5, figs. 129, 130.

Textularia earlandi Parker 1952, p. 458, pl. 2, figs. 4-5. Note: The species has been determined as *Textularia tenuissima* Earland 1933 by authors.

**Textularia pseudogramen* Chapman and Parr 1937, p. 153.

Tiphotrocha comprimata (Cushman and Bronniman) = *Trochammina comprimata* Cushman and Bronniman 1948: p. 41, pl. 8, figs. 1–3.

Triloculina oblonga (Montagu) = *Vermiculum oblongum* Montagu 1803, p. 522, pl. 14, fig. 9.

Triloculina trigonula (Lamarck) = *Miliolites trigonula* Lamarck 1804, p. 351, pl. 17, figs. 4a-c.

Trochammina advena Cushman 1922, p. 20, pl. 1, figs. 2-4.

Trochamminita astrifica Rhumbler = *Trochammina squamata* Jones and Parker var. *astrifica* Rhumbler 1938, p. 188, figs. 29-31.

Trochammina inflata (Montagu) = *Nautilus inflatus* Montagu, 1808, p. 81, pl. 18, fig. 3.

Trochamminita irregularis Cushman and Brönnimann 1948, p. 17, pl. 4, fig. 1-3.

Trochammina squamata Jones and Parker 1860, p. 304.

Wiesnerella auriculata (Egger) = *Planispirina auriculata* Egger, 1893, p. 245, pl. 3, figs. 13-15.

Supplements

Supplement Table 1. Sediments and macrofauna on the Esteiro do Ancão backbarrier beach transect.
Supplement Table 2. Temperature and salinity measurements of Esteiro do Ancão surface waters.
Supplement Table 3. Tide gauge records from Ponte da Praia de Faro.
Supplement Table 4. Current measurements at Ponte da Praia de Faro.
Supplement Table 5. Foraminiferal census data 2014.
Supplement Table 6. Foraminiferal census data 2015.
Supplement Table 7. Foraminiferal census data 2016.
Supplement Table 8. Foraminiferal census data 2017.
Supplement Table 9. Foraminiferal census data from the 30-m monitoring site.
Supplement Table 10. Nutrient measurements of Esteiro do Ancão surface waters.

Supplement Table 1. Observations of sediment grain size, structures, macroorganisms and macrophyte occurrences along the Esteiro do Ancão backbarrier beach transect. Distances are given in meters from transect zero.

2013	2014	2015	2016	2017	2018	2019
0 m: medium to coarse sand with crab shell debris, erosional brink	0.4 m: medium sand, erosional brink	0.3 m: medium sand, erosional brink	-0.8-0 m: medium sand with bivalve shells, brink with debris seam	-0.8 - -0.1 m: medium sand, brink, debris seam	-0.9 m: medium sand, erosional brink, vegetation boundary at -0.38 m	-0.7 m: medium sand, erosional brink
3.2 m: debris seam	2.2-2.9 m: medium sand, debris seam	3.6 m: medium to coarse sand, change in composition	0-6.5 m: medium to coarse sand with heavy mineral placers	-0.1-3.35 m: medium to coarse sand with heavy mineral placers and debris seams	0-4.2 m: medium to coarse sand with heavy mineral placers and debris seams	-0.7-2.3 m: medium sand, debris seams
8.7-14.3 m: medium to coarse sand, water level marks of coarse sand with bivalve shells and pebbles	9.2-15.5 m: medium to coarse sand, water level marks	3.6-12.25 m: medium to coarse sand with pebbles and shell debris, truck trail, current ripples, comet marks	6.5-12.4 m: coarse sand, ripples, pebble lag, dewatering rills	3.35-13.1 m: medium to coarse sand with shells an pebbles, flute marks, comet marks, ripples	4.2-16 m: medium to coarse sand with water level marks	2.3-17.4 m: coarse sand with pebbles and shells, water level marks
15.5-21 m: coarse sand, mega-ripples, *Ulva*	15.5 m: pebbly coarse sand, seeps, *Littorina*	12.25-14.5 m: coarse sand wih large pebbles, water level marks, seeps	12.4-19 m: pebbly coarse sand, water level marks	13.1-19.1 m: pebbly coarse sand with shell debris, water level marks, dewatering rills, scattered *Ulva*	16-19.5 m: medium to coarse sand with pebbles, dewatering rills	17.4-21 m: coarse sand with pebbles, dewatering rills, green algae
19 m: pebbles with coarse sand and shells, seeps, *Littorina*	19.5 m: pebbles with coarse sand and shell debris, megaripples, dewatering rills, *Ulva,* small oysters	14.5-19.8 m: pebbly coarse sand with cobbles and shell debris, mega-ripples, dewater-ing rills, abundant *Littorina,* scattered *Ulva*	19-21 m: coarse sand - pebbles, scattered Ulva	19.1-26.8 m: pebbly sand with shell debris, firmgrounds 0,5-1 m ø, with hydrozoans, serpulids, oysters, *Ulva* on top, abundant *Littorina,* seeps	19.5-26 m: pebbly coarse sand with shell debris, dewatering rills, *Ulva,* green algae small hydroid colonies, *Littorina*	21-28.2 m: coarse sand with pebbles, dewatering rills, large *Ulva,* green algae, balanids and serpulids on pebbles
27-36 m: firmgrounds 1-3 m ø, oval shaped, with long axis perpendicular to the slope, oysters, balanids, gastropods, *Ulva* on top	26-32 m: coarse sand with shell debris and pebbles, firmgrounds 0.1-0.2 m ø, serpulids, bryozoans, oysters, *Ulva* on top, also tunicates, sea anemonas	19.8-36.7 m: medium to coarse sand with pebbles and shell debris. 22.5-33 m: oval firmgrounds 1-2 m ø, perpendicular to the slope, serpulids, hydroids, oysters, gastropods, *Ulva* on top	21-35 m: coarse sand - pebbles, firmgrounds 0.5 m ø and 3-5 cm high, oysters, bala-nids, hydroids, serpulids, Ulva on top; tube-building polychaet colonies	26.8-34 m: medium to coarse sand, tube-building polychaet colonies 0.2-0.7 m ø, sponges, nudibranches, *Ulva*	26-32.2 m: medium to coarse sand with pebbles and shell debris, dense colonies of tube-building polychaets, *Ulva*	28.2-33.2 m: coarse sand with pebbles, colonies of tube-building polychaets, crabs and hermit crabs
not examined	32-38.1 m: pebbly coarse sand, scattered *Ulva*	36.7-37 m: silty coarse sand	35-36 m: muddy coarse sand	34-35.2 m: muddy coarse sand with fragments of polychaet tubes, *Bittium,* hydroids	32.2-35.6 m: coarse sand - pebbles with shell debris, *Ulva* in patches, polychaet tubes, hermit crabs	33.2-35.2 m: coarse sand with pebble lag, oyster shells, balanids, *Ulva*
not examined	38.1-(50 m): very soft mud, *Zostera*	37-(45 m): mud with *Zostera,* in beween sponges, sea cucumbers, large dark-brown nudibranches (*Aplysia*).	36-(43 m): sandy mud with *Zostera,* tunicates	35.2-(43 m): sandy mud with *Zostera*	35.6-(43 m): sandy mud with *Zostera,* tunicates, *Littorina*	35.2-(44 m): sandy mud with Zostera, green algae, hermit crabs, nudibranches (*Aplysia*)

Supplement Table 2. Temperature and salinity measurements of Esteiro do Ancão surface water.

Year	Date	Time	Tide	Location	Instrument	Temperature (°C)	Salinity
2013	15.04.13		flood	Esteiro do Ancão transect	SM-11 (LF320)	23,6	35,2
2014	30.04.14		flood	Esteiro do Ancão transect	LF320	25,7	35,5
	01.05.14	18:35	ebb	Ponte da Praia de Faro	LF320	20,0	35,8
2015	22.04.15	16:44	ebb	Ponte da Praia de Faro	LF320	19,7	36,2
	24.04.15	10:27	ebb	Ponte da Praia de Faro	LF320	19,3	36,4
2016	03.05.16	09:18	flood	Ponte da Praia de Faro	Cond3210	17,8	36,7
	05.05.16	11:25	flood	Aeromar slipway	Cond3210	18,4	36,5
	07.05.16	08:16	ebb	Aeromar slipway	Cond3210	17,0	35,8
	09.05.16	13:14	flood	Aeromar slipway	Cond3210	19,0	35,0
2017	21.04.17	16:43	ebb	Aeromar slipway	Cond3210	18,3	36,2
	28.04.17	18:15	ebb	Aeromar slipway	Cond3210	19,1	36,0
	29.04.17	11:35	ebb	Aeromar slipway	Cond3210	21,1	36,0
	29.04.17	13:30	flood	Aeromar slipway	Cond3210	20,1	35,7
	29.04.17	14:29	flood	Aeromar slipway	Cond3210	20,2	36,1
	29.04.17	15:26	flood	Aeromar slipway	Cond3210	19,9	36,3
	29.04.17	16:30	flood	Aeromar slipway	Cond3210	20,1	36,3
	29.04.17	17:30	flood	Aeromar slipway	Cond3210	19,7	36,2
	29.04.17	18:15	ebb	Aeromar slipway	Cond3210	20,2	36,2
2018	03.05.18	12:20	flood	Esteiro do Ancão transect	Cond3210	21,0	34,4
	04.05.18	10:05	ebb	Ponte da Praia de Faro	Cond3210	18,0	36,3
	06.05.18	12:20	ebb	Ponte da Praia de Faro	Cond3210	21,0	36,1
	08.05.18	12:36	ebb	Ponte da Praia de Faro	Cond3210	21,8	36,2
2019	02.05.19	07:40	ebb	Ponte da Praia de Faro	Cond3210	21,6	37,0
	05.05.19	08:20	ebb	Ponte da Praia de Faro	Cond3210	20,9	37,0
	07.05.19	10:20	ebb	Ponte da Praia de Faro	Cond3210	19,4	37,1
	09.05.19	11:55	ebb	Ponte da Praia de Faro	Cond3210	20,5	37,0
	29.11.19	09:00	ebb	Ponte da Praia de Faro	LF320	15,4	36,3
	29.11.19	09:00	ebb	Ponte da Praia de Faro	LF320	15,7	36,0
	29.11.19	09:00	ebb	Ponte da Praia de Faro	LF320	15,4	36,2
2020	20.08.20	14:50	flood	Mid of boardwalk to Praia	LF320	25,8	37,3
	20.08.20	15:10	flood	Mid of boardwalk to Praia	LF320	25,1	37,2
	20.08.20	15:30	flood	Mid of boardwalk to Praia	LF320	24,0	37,1
	20.08.20	15:50	flood	Mid of boardwalk to Praia	LF320	23,3	37,0
	20.08.20	16:10	flood	Mid of boardwalk to Praia	LF320	22,9	37,0
	20.08.20	16:30	flood	Mid of boardwalk to Praia	LF320	24,1	37,0
	20.08.20	17:40	ebb	Mid of boardwalk to Praia	LF320	23,3	36,9
	20.08.20	18:00	ebb	Mid of boardwalk to Praia	LF320	23,1	36,9
	20.08.20	18:20	ebb	Mid of boardwalk to Praia	LF320	22,6	36,6
	20.08.20	18:40	ebb	Mid of boardwalk to Praia	LF320	22,9	36,7
					Mean (2013-2019):	20,1	36,1
					Maximum:	25,7	37,1
					Minimum:	17,0	34,4
					Standard deviation:	1,8	0,6
					Mean ebb (2013-2019):	19,9	36,4
					Mean flood (2013-2019):	20,5	35,8

Supplement Table 3. Tide gauge records from Ponte da Praia de Faro and comparison with forecasts of Instituto Hidrografico (IH)

Tide	Date and Time, Ponte da Praia de Faro (WET)	Level (m POD)	Tidal amplitude (m)	Flood/ebb period	Mean Tidal Level (m POD)	Date and time Barra de Faro-Olhão, IH (WET)	Predicted water level (m POD)	Difference observation - prediction (m)	Time lag (observation - prediction)
Low Tide	12.04.13 10:16	-1,24				12.04.13 09:20	-1,3	0,1	0:56
High Tide	12.04.13 16:36	1,43	2,67	06:20		12.04.13 15:48	1,3	0,1	0:48
Low Tide	12.04.13 22:36	-1,27	2,7	06:00		12.04.13 21:39	-1,3	0,0	0:57
High Tide	13.04.13 04:56	1,33	2,6	06:20		13.04.13 04:06	1,2	0,1	0:50
Low Tide	13.04.13 10:46	-1,13	2,46	05:50		13.04.13 09:50	-1,2	0,1	0:56
High Tide	13.04.13 17:06	1,38	2,51	06:20		13.04.13 16:22	1,2	0,2	0:44
Low Tide	13.04.13 23:06	-1,14	2,52	06:00		13.04.13 22:12	-1,2	0,1	0:54
High Tide	14.04.13 05:26	1,23	2,37	06:20		14.04.13 04:39	1,0	0,2	0:47
Low Tide	14.04.13 11:06	-0,98	2,21	05:40		14.04.13 10:21	-1,1	0,1	0:45
High Tide	14.04.13 17:46	1,27	2,25	06:40		14.04.13 16:55	1,0	0,3	0:51
Low Tide	14.04.13 23:36	-1,01	2,28	05:50	0,20	14.04.13 22:46	-1,0	0,0	0:50
High Tide	15.04.13 05:56	1,04	2,05	06:20		15.04.13 05:13	0,8	0,2	0:43
Low Tide	29.04.14 09:40	-1,16				29.04.14 08:14	-1,5	0,3	1:26
High Tide	29.04.14 15:45	1,64	2,8	06:05		29.04.14 14:39	1,4	0,2	1:06
Low Tide	29.04.14 22:00	-1,18	2,82	06:15		29.04.14 20:35	-1,5	0,3	1:25
High Tide	30.04.14 04:10	1,6	2,78	06:10		30.04.14 03:01	1,4	0,2	1:09
Low Tide	30.04.14 10:15	-1,13	2,73	06:05		30.04.14 08:51	-1,4	0,3	1:24
High Tide	30.04.14 16:25	1,63	2,76	06:10		30.04.14 15:20	1,4	0,2	1:05
Low Tide	30.04.14 22:40	-1,14	2,77	06:15		30.04.14 21:14	-1,4	0,3	1:26
High Tide	01.05.14 04:45	1,49	2,63	06:05		01.05.14 03:41	1,3	0,2	1:04
Low Tide	01.05.14 10:45	-1,1	2,59	06:00		01.05.14 09:27	-1,3	0,2	1:18
High Tide	01.05.14 17:00	1,54	2,64	06:15		01.05.14 15:59	1,3	0,2	1:01
Low Tide	01.05.14 23:10	-1,13	2,67	06:10		01.05.14 21:52	-1,3	0,2	1:18
High Tide	02.05.14 05:25	1,37	2,5	06:15		02.05.14 04:19	1,1	0,3	1:06
Low Tide	02.05.14 11:10	-1	2,37	05:45		02.05.14 10:02	-1,2	0,2	1:08
High Tide	02.05.14 17:35	1,46	2,46	06:25		02.05.14 16:37	1,2	0,3	0:58
Low Tide	02.05.14 23:40	-1	2,46	06:05		02.05.14 22:30	-1,2	0,2	1:10
High Tide	03.05.14 05:55	1,26	2,26	06:15		03.05.14 04:57	1,0	0,3	0:58
Low Tide	03.05.14 11:40	-0,88	2,14	05:45		03.05.14 10:37	-1,0	0,1	1:03
High Tide	03.05.14 18:10	1,32	2,2	06:30		03.05.14 17:16	1,0	0,3	0:54
Low Tide	04.05.14 00:10	-0,88	2,2	06:00		03.05.14 23:10	-1,0	0,1	1:00
High Tide	04.05.14 06:30	1,11	1,99	06:20		04.05.14 05:37	0,8	0,3	0:53
Low Tide	04.05.14 12:05	-0,73	1,84	05:35		04.05.14 11:15	-0,8	0,1	0:50
High Tide	04.05.14 18:50	1,18	1,91	06:45		04.05.14 17:57	0,9	0,3	0:53
Low Tide	05.05.14 00:45	-0,72	1,9	05:55		04.05.14 23:55	-0,8	0,1	0:50
High Tide	05.05.14 07:10	0,95	1,67	06:25		05.05.14 06:22	0,6	0,4	0:48
Low Tide	05.05.14 12:45	-0,56	1,51	05:35		05.05.14 12:00	-0,7	0,1	0:45
High Tide	05.05.14 19:25	1,06	1,62	06:40		05.05.14 18:45	0,8	0,3	0:40
Low Tide	06.05.14 01:25	-0,59	1,65	06:00		06.05.14 00:52	-0,7	0,1	0:33
High Tide	06.05.14 08:05	0,87	1,46	06:40		06.05.14 07:19	0,5	0,4	0:46
Low Tide	06.05.14 13:35	-0,4	1,27	05:30	0,28	06.05.14 13:00	-0,5	0,1	0:35
High Tide	16.04.15 13:40	1,55				16.04.15 12:43	1,3	0,3	0:57
Low Tide	16.04.15 19:45	-1,15	2,7	06:05		16.04.15 18:41	-1,4	0,3	1:04
High Tide	17.04.15 01:55	1,79	2,94	06:10		17.04.15 01:04	1,5	0,3	0:51
Low Tide	17.04.15 08:30	-1,2	2,99	06:35		17.04.15 07:08	-1,6	0,4	1:22
High Tide	17.04.15 14:30	1,74	2,94	06:00		17.04.15 13:30	1,5	0,2	1:00
Low Tide	17.04.15 20:50	-1,19	2,93	06:20		17.04.15 19:27	-1,6	0,4	1:23
High Tide	18.04.15 02:45	1,92	3,11	05:55		18.04.15 01:52	1,6	0,3	0:53
Low Tide	18.04.15 09:25	-1,25	3,17	06:40		18.04.15 07:52	-1,7	0,5	1:33
High Tide	18.04.15 15:15	1,79	3,04	05:50		18.04.15 14:16	1,6	0,2	0:59
Low Tide	18.04.15 21:40	-1,3	3,09	06:25		18.04.15 20:11	-1,7	0,4	1:29
High Tide	19.04.15 03:35	1,88	3,18	05:55		19.04.15 02:39	1,7	0,2	0:56
Low Tide	19.04.15 10:05	-1,26	3,14	06:30		19.04.15 08:34	-1,7	0,4	1:31
High Tide	19.04.15 15:55	1,86	3,12	05:50		19.04.15 15:00	1,6	0,3	0:55
Low Tide	19.04.15 22:30	-1,28	3,14	06:35		19.04.15 20:54	-1,7	0,4	1:36
High Tide	20.04.15 04:20	1,87	3,15	05:50		20.04.15 03:24	1,6	0,3	0:56
Low Tide	20.04.15 10:50	-1,21	3,08	06:30		20.04.15 09:14	-1,6	0,4	1:36
High Tide	20.04.15 16:40	1,79	3	05:50		20.04.15 15:44	1,6	0,2	0:56
Low Tide	20.04.15 23:10	-1,28	3,07	06:30		20.04.15 21:36	-1,6	0,3	1:34
High Tide	21.04.15 05:05	1,74	3,02	05:55		21.04.15 04:08	1,5	0,2	0:57
Low Tide	21.04.15 11:20	-1,09	2,83	06:15		21.04.15 09:55	-1,5	0,4	1:25
High Tide	21.04.15 17:25	1,8	2,89	06:05		21.04.15 16:28	1,5	0,3	0:57
Low Tide	21.04.15 23:45	-1,1	2,9	06:20		21.04.15 22:19	-1,5	0,4	1:26
High Tide	22.04.15 05:45	1,56	2,66	06:00		22.04.15 04:52	1,3	0,3	0:53
Low Tide	22.04.15 11:50	-1,08	2,64	06:05		22.04.15 10:35	-1,3	0,2	1:15
High Tide	22.04.15 18:05	1,51	2,59	06:15		22.04.15 17:12	1,3	0,2	0:53
Low Tide	23.04.15 00:15	-1,1	2,61	06:10		22.04.15 23:04	-1,2	0,1	1:11
High Tide	23.04.15 06:30	1,29	2,39	06:15		23.04.15 05:38	1,0	0,3	0:52
Low Tide	23.04.15 12:15	-0,92	2,21	05:45		23.04.15 11:18	-1,0	0,1	0:57
High Tide	23.04.15 18:45	1,32	2,24	06:30		23.04.15 17:59	1,1	0,2	0:46
Low Tide	24.04.15 00:45	-0,95	2,27	06:00		23.04.15 23:54	-1,0	0,1	0:51
High Tide	24.04.15 07:15	1,06	2,01	06:30		24.04.15 06:28	0,8	0,3	0:47

Tide	Date and Time, Ponte da Praia de Faro (WET)	Level (m POD)	Tidal amplitude (m)	Flood/ebb period	Mean Tidal Level (m POD)	Date and time Barra de Faro-Olhão, IH (WET)	Predicted water level (m POD)	Difference observation - prediction (m)	Time lag (observation - prediction)
Low Tide	24.04.15 12:45	-0,76	1,82	05:30		24.04.15 12:06	-0,8	0,0	0:39
High Tide	24.04.15 19:40	1,1	1,86	06:55		24.04.15 18:52	0,9	0,2	0:48
Low Tide	25.04.15 01:25	-0,74	1,84	05:45		25.04.15 00:55	-0,8	0,1	0:30
High Tide	25.04.15 08:10	0,87	1,61	06:45		25.04.15 07:26	0,6	0,3	0:44
Low Tide	25.04.15 13:30	-0,55	1,42	05:20		25.04.15 13:10	-0,6	0,0	0:20
High Tide	25.04.15 20:35	0,97	1,52	07:05		25.04.15 19:55	0,7	0,3	0:40
Low Tide	26.04.15 02:20	-0,55	1,52	05:45		26.04.15 02:14	-0,6	0,0	0:06
High Tide	26.04.15 09:10	0,81	1,36	06:50		26.04.15 08:36	0,5	0,3	0:34
Low Tide	26.04.15 14:50	-0,43	1,24	05:40		26.04.15 14:36	-0,5	0,1	0:14
High Tide	26.04.15 21:50	0,87	1,3	07:00		26.04.15 21:07	0,6	0,3	0:43
Low Tide	27.04.15 03:40	-0,56	1,43	05:50		27.04.15 03:36	-0,6	0,0	0:04
High Tide	27.04.15 10:35	0,76	1,32	06:55		27.04.15 09:52	0,5	0,3	0:43
Low Tide	27.04.15 16:15	-0,48	1,24	05:40		27.04.15 16:00	-0,5	0,0	0:15
High Tide	27.04.15 22:55	0,87	1,35	06:40	0,31	27.04.15 22:19	0,7	0,2	0:36
Low Tide	28.04.15 04:55	-0,64	1,51	06:00		28.04.15 04:41	-0,7	0,1	0:14
High Tide	03.05.16 12:15	1,44				03.05.16 11:48	1,1	0,3	0:27
Low Tide	03.05.16 17:55	-1,01	2,45	05:40		03.05.16 17:47	-1,1	0,1	0:08
High Tide	04.05.16 00:35	1,68	2,69	06:40		04.05.16 00:09	1,3	0,4	0:26
Low Tide	04.05.16 06:30	-1,24	2,92	05:55		04.05.16 06:15	-1,4	0,2	0:15
High Tide	04.05.16 13:05	1,69	2,93	06:35		04.05.16 12:38	1,3	0,4	0:27
Low Tide	04.05.16 19:00	-1,27	2,96	05:55		04.05.16 18:36	-1,4	0,1	0:24
High Tide	05.05.16 01:25	1,91	3,18	06:25		05.05.16 00:59	1,5	0,4	0:26
Low Tide	05.05.16 07:30	-1,4	3,31	06:05		05.05.16 07:02	-1,6	0,2	0:28
High Tide	05.05.16 13:50	1,98	3,38	06:20		05.05.16 13:26	1,5	0,5	0:24
Low Tide	05.05.16 19:55	-1,37	3,35	06:05		05.05.16 19:23	-1,6	0,2	0:32
High Tide	06.05.16 02:15	2,1	3,47	06:20		06.05.16 01:48	1,6	0,5	0:27
Low Tide	06.05.16 08:30	-1,48	3,58	06:15		06.05.16 07:47	-1,7	0,2	0:43
High Tide	06.05.16 14:40	2,06	3,54	06:10		06.05.16 14:13	1,6	0,5	0:27
Low Tide	06.05.16 20:50	-1,51	3,57	06:10		06.05.16 20:09	-1,7	0,2	0:41
High Tide	07.05.16 03:05	2,13	3,64	06:15		07.05.16 02:36	1,6	0,5	0:29
Low Tide	07.05.16 09:15	-1,47	3,6	06:10		07.05.16 08:30	-1,7	0,2	0:45
High Tide	07.05.16 15:30	2,21	3,68	06:15		07.05.16 14:59	1,7	0,5	0:31
Low Tide	07.05.16 21:45	-1,39	3,6	06:15		07.05.16 20:54	-1,8	0,4	0:51
High Tide	08.05.16 03:50	2,31	3,7	06:05		08.05.16 03:23	1,6	0,7	0:27
Low Tide	08.05.16 10:00	-1,29	3,6	06:10		08.05.16 09:13	-1,7	0,4	0:47
High Tide	08.05.16 16:15	2,24	3,53	06:15		08.05.16 15:45	1,6	0,6	0:30
Low Tide	08.05.16 22:25	-1,37	3,61	06:10		08.05.16 21:39	-1,7	0,3	0:46
High Tide	09.05.16 04:45	2,08	3,45	06:20	0,46	09.05.16 04:11	1,5	0,6	0:34
Low Tide	09.05.16 10:40	-1,23	3,31	05:55		09.05.16 09:57	-1,5	0,3	0:43
High Tide	23.04.17 00:20	1,5				22.04.17 23:54	1,0	0,5	0:26
Low Tide	23.04.17 06:10	-0,91	2,41	05:50		23.04.17 06:01	-1,1	0,2	0:09
High Tide	23.04.17 13:00	1,51	2,42	06:50		23.04.17 12:22	1,1	0,4	0:38
Low Tide	23.04.17 18:35	-0,89	2,4	05:35		23.04.17 18:18	-1,1	0,2	0:17
High Tide	24.04.17 01:10	1,7	2,59	06:35		24.04.17 00:40	1,2	0,5	0:30
Low Tide	24.04.17 07:05	-1,16	2,86	05:55		24.04.17 06:43	-1,4	0,2	0:22
High Tide	24.04.17 13:45	1,73	2,89	06:40		24.04.17 13:06	1,3	0,4	0:39
Low Tide	24.04.17 19:30	-1,16	2,89	05:45		24.04.17 19:01	-1,4	0,2	0:29
High Tide	25.04.17 02:00	1,91	3,07	06:30		25.04.17 01:25	1,4	0,5	0:35
Low Tide	25.04.17 08:00	-1,36	3,27	06:00		25.04.17 07:25	-1,6	0,2	0:35
High Tide	25.04.17 14:25	1,87	3,23	06:25		25.04.17 13:49	1,5	0,4	0:36
Low Tide	25.04.17 20:20	-1,38	3,25	05:55		25.04.17 19:43	-1,6	0,2	0:37
High Tide	26.04.17 02:45	2,01	3,39	06:25		26.04.17 02:09	1,6	0,4	0:36
Low Tide	26.04.17 08:50	-1,48	3,49	06:05		26.04.17 08:06	-1,7	0,2	0:44
High Tide	26.04.17 15:10	1,98	3,46	06:20		26.04.17 14:32	1,6	0,4	0:38
Low Tide	26.04.17 21:10	-1,55	3,53	06:00		26.04.17 20:26	-1,7	0,2	0:44
High Tide	27.04.17 03:30	2,07	3,62	06:20		27.04.17 02:54	1,6	0,5	0:36
Low Tide	27.04.17 09:40	-1,55	3,62	06:10		27.04.17 08:47	-1,7	0,2	0:53
High Tide	27.04.17 15:55	2,06	3,61	06:15		27.04.17 15:16	1,6	0,5	0:39
Low Tide	27.04.17 22:00	-1,53	3,59	06:05		27.04.17 21:08	-1,7	0,2	0:52
High Tide	28.04.17 04:15	2,11	3,64	06:15		28.04.17 03:39	1,6	0,5	0:36
Low Tide	28.04.17 10:15	-1,46	3,57	06:00		28.04.17 09:29	-1,7	0,2	0:46
High Tide	28.04.17 16:35	2,09	3,55	06:20		28.04.17 16:01	1,6	0,5	0:34
Low Tide	28.04.17 22:40	-1,47	3,56	06:05		28.04.17 21:52	-1,7	0,2	0:48
High Tide	29.04.17 05:00	1,99	3,46	06:20		29.04.17 04:25	1,5	0,5	0:35
Low Tide	29.04.17 10:55	-1,35	3,34	05:55		29.04.17 10:12	-1,5	0,2	0:43
High Tide	29.04.17 17:20	1,9	3,25	06:25		29.04.17 16:47	1,5	0,4	0:33
Low Tide	29.04.17 23:15	-1,43	3,33	05:55		29.04.17 22:39	-1,5	0,1	0:36
High Tide	30.04.17 05:50	1,68	3,11	06:35		30.04.17 05:14	1,3	0,4	0:36
Low Tide	30.04.17 11:25	-1,27	2,95	05:35		30.04.17 10:58	-1,3	0,0	0:27
High Tide	30.04.17 18:05	1,66	2,93	06:40		30.04.17 17:37	1,3	0,4	0:28
Low Tide	30.04.17 23:55	-1,31	2,97	05:50		30.04.17 23:31	-1,3	0,0	0:24
High Tide	01.05.17 06:40	1,37	2,68	06:45		01.05.17 06:09	1,1	0,3	0:31

Tide	Date and Time, Ponte da Praia de Faro (WET)	Level (m POD)	Tidal amplitude (m)	Flood/ebb period	Mean Tidal Level (m POD)	Date and time Barra de Faro-Olhão, IH (WET)	Predicted water level (m POD)	Difference observation - prediction (m)	Time lag (observation - prediction)
Low Tide	01.05.17 12:05	-1,02	2,39	05:25		01.05.17 11:50	-1,0	0,0	0:15
High Tide	01.05.17 19:05	1,45	2,47	07:00		01.05.17 18:34	1,1	0,4	0:31
Low Tide	02.05.17 00:45	-1,01	2,46	05:40		02.05.17 00:33	-1,1	0,1	0:12
High Tide	02.05.17 07:40	1,21	2,22	06:55	0,38	02.05.17 07:12	0,9	0,3	0:28
Low Tide	02.05.17 13:05	-0,68	1,89	05:25		02.05.17 12:54	-0,8	0,1	0:11

Mean tidal level	
mean:	0,33
weighed mean:	0,34
weighed mean before new inlet:	0,29
weighed mean after new inlet:	0,41

Tidal amplitude	
mean:	2,69
max:	3,70
min:	1,24
mean before inlet relocation:	2,34
mean after inlet relocation:	3,17

Flood period	
mean:	6:23
max:	7:05
min:	5:50
mean before new inlet:	6:20
mean after new inlet:	6:27

Ebb period	
mean:	5:58
max:	6:40
min:	5:20
mean before new inlet:	6:00
mean after new inlet:	5:55

Difference observation - prediction (m)	
mean High Tide:	0,33
mean High Tide before new inlet:	0,25
mean High Tide after new inlet:	0,45
mean Low Tide:	0,19
mean Low Tide before new inlet:	0,19
mean Low Tide after new inlet:	0,19

Time lag (observation - prediction)	
mean High Tide:	0:43
mean High Tide before new inlet:	0:52
mean High Tide after new inlet:	0:31
mean Low Tide:	0:48
mean Low Tide before new inlet:	1:00
mean Low Tide after new inlet:	0:33

Supplement Table 4. Current measurements in Esteiro do Ancão main channel at Ponte da Praia de Faro.

Deployment start, date and time (WET)	Flow direction (in/out)	Instrument hight (m POD)	Immersion depth (m)	Current velocity ($m\ s^{-1}$)	Tidal amplitude (m)	Mean current 1/2 tide ($m\ s^{-1}$)	Maximum current 1/2 tide ($m\ s^{-1}$)	Standard deviation (±$m\ s^{-1}$)
05.05.14 08:00	out	-0,18	1,00	0,51	1,51	0,468	0,630	0,153
05.05.14 08:08	out	-1,40	2,18	0,51				
05.05.14 08:14	out	-2,32	3,08	0,42				
05.05.14 09:35	out	-0,52	0,93	0,63				
05.05.14 09:40	out	-1,58	1,96	0,58				
05.05.14 09:46	out	-2,41	2,76	0,43				
05.05.14 11:03	out	-0,99	0,87	0,63				
05.05.14 11:09	out	-1,75	1,60	0,54				
05.05.14 12:22	out	-2,05	1,53	0,25				
05.05.14 12:29	out	-2,32	1,78	0,17				
05.05.14 13:34	in	-1,51	1,12	0,29	1,62	0,349	0,567	0,129
05.05.14 13:40	in	-1,69	1,33	0,29				
05.05.14 14:38	in	-1,41	1,29	0,33				
05.05.14 14:44	in	-2,14	2,04	0,16				
05.05.14 15:50	in	-0,95	1,12	0,49				
05.05.14 15:56	in	-1,72	1,92	0,47				
05.05.14 16:03	in	-2,67	2,91	0,32				
05.05.14 17:25	in	-0,37	1,00	0,57				
05.05.14 17:30	in	-2,12	2,78	0,29				
05.05.14 17:35	in	-3,31	3,99	0,15				
05.05.14 18:36	in	-0,15	1,10	0,46				
05.05.14 18:41	in	-1,65	2,62	0,37				
21.04.15 05:36	out	0,41	1,21	0,73	2,83	0,712	0,893	0,202
21.04.15 05:45	out	-0,25	1,81	0,77				
21.04.15 05:57	out	-1,50	2,96	0,80				
21.04.15 06:46	out	0,01	1,15	0,86				
21.04.15 06:54	out	-1,01	2,11	0,78				
21.04.15 07:00	out	-1,70	2,77	0,76				
21.04.15 07:05	out	-1,84	2,89	0,77				
21.04.15 08:08	out	-0,56	1,18	0,85				
21.04.15 08:17	out	-0,44	0,97	0,88				
21.04.15 08:24	out	-1,00	1,48	0,83				
21.04.15 08:33	out	-2,89	3,29	0,39				
21.04.15 09:36	out	-1,53	1,35	0,89				
21.04.15 09:43	out	-2,93	2,69	0,21				
21.04.15 09:52	out	-1,49	1,18	0,83				
21.04.15 10:43	out	-2,11	1,25	0,65				
21.04.15 10:47	out	-2,23	1,31	0,39				
24.04.15 07:34	out	-1,81	2,84	0,17	1,82	0,459	0,733	0,205
24.04.15 07:41	out	-0,74	1,75	0,31				
24.04.15 07:47	out	-2,09	3,08	0,34				
24.04.15 07:53	out	-0,07	1,02	0,49				
24.04.15 08:48	out	-2,47	3,16	0,25				
24.04.15 08:54	out	-1,19	1,85	0,58				
24.04.15 09:01	out	-0,40	1,02	0,61				
24.04.15 10:04	out	-2,04	2,30	0,67				

Deployment start, date and time (WET)	Flow direction (in/out)	Instrument hight (m POD)	Immersion depth (m)	Current velocity ($m\ s^{-1}$)	Tidal amplitude (m)	Mean current 1/2 tide ($m\ s^{-1}$)	Maximum current 1/2 tide ($m\ s^{-1}$)	Standard deviation ($\pm m\ s^{-1}$)
24.04.15 10:10	out	-1,20	1,42	0,72				
24.04.15 10:16	out	-0,88	1,05	0,73				
24.04.15 11:18	out	-2,43	2,15	0,28				
24.04.15 11:26	out	-1,37	1,04	0,60				
24.04.15 12:35	out	-1,92	1,18	0,21				
24.04.15 12:42	in	-1,86	1,11	0,13	1,86	0,355	0,626	0,179
24.04.15 13:35	in	-1,73	1,19	0,21				
24.04.15 14:35	in	-2,10	1,84	0,14				
24.04.15 14:41	in	-1,47	1,23	0,27				
24.04.15 15:39	in	-2,16	2,19	0,28				
24.04.15 15:45	in	-1,12	1,18	0,45				
24.04.15 16:35	in	-2,30	2,63	0,15				
24.04.15 16:42	in	-1,25	1,60	0,54				
24.04.15 16:47	in	-0,64	1,03	0,55				
24.04.15 17:37	in	-2,31	2,97	0,37				
24.04.15 17:43	in	-1,07	1,77	0,62				
24.04.15 17:49	in	-0,32	1,04	0,63				
24.04.15 18:49	in	-2,11	3,12	0,15				
24.04.15 18:55	in	-1,36	2,40	0,43				
24.04.15 19:01	in	-0,02	1,07	0,42				
23.04.17 06:35	in	-1,43	0,61	0,14	2,42	0,417	0,78	0,26
23.04.17 06:44	in	-1,92	1,15	0,18				
23.04.17 07:32	in	-1,14	0,66	0,26				
23.04.17 07:39	in	-2,04	1,59	0,17				
23.04.17 07:46	in	-1,71	1,30	0,23				
23.04.17 08:28	in	-2,06	1,90	0,25				
23.04.17 08:35	in	-1,55	1,43	0,49				
23.04.17 08:42	in	-0,75	0,68	0,62				
23.04.17 09:30	in	-2,43	2,73	0,39				
23.04.17 09:36	in	-0,99	1,35	0,77				
23.04.17 09:43	in	-0,21	0,62	0,76				
23.04.17 10:32	in	-2,55	3,32	0,18				
23.04.17 10:38	in	-0,26	1,07	0,78				
23.04.17 10:45	in	-0,75	1,62	0,77				
23.04.17 11:29	in	-2,49	3,65	0,17				
23.04.17 11:36	in	-0,97	2,19	0,74				
23.04.17 11:47	in	0,26	1,03	0,77				
23.04.17 12:35	in	-2,24	3,73	0,18				
23.04.17 12:43	in	-0,85	2,35	0,28				
23.04.17 12:50	in	0,43	1,07	0,22				
23.04.17 13:32	out	-2,15	3,56	0,15	2,4	0,565	0,884	0,256
23.04.17 13:40	out	-0,51	1,88	0,55				
23.04.17 13:47	out	0,54	0,79	0,66				
23.04.17 14:33	out	-2,97	4,01	0,34				
23.04.17 14:41	out	-1,09	2,09	0,79				
23.04.17 14:48	out	0,32	0,64	0,75				
23.04.17 15:32	out	-2,31	2,93	0,58				
23.04.17 15:40	out	-0,37	0,94	0,83				

Deployment start, date and time (WET)	Flow direction (in/out)	Instrument hight (m POD)	Immersion depth (m)	Current velocity (m s^{-1})	Tidal amplitude (m)	Mean current 1/2 tide (m s^{-1})	Maximum current 1/2 tide (m s^{-1})	Standard deviation (±m s^{-1})
23.04.17 15:47	out	-1,01	1,52	0,80				
23.04.17 16:30	out	-2,17	2,29	0,75				
23.04.17 16:38	out	-0,68	0,71	0,88				
23.04.17 17:32	out	-2,42	1,88	0,35				
23.04.17 17:39	out	-1,28	0,68	0,72				
23.04.17 17:47	out	-1,95	1,29	0,60				
23.04.17 18:29	out	-2,09	1,21	0,17				
23.04.17 18:32	out	-1,88	1,00	0,13				
29.04.17 12:05	in	-2,11	1,40	0,16	3,25	0,554	0,847	0,282
29.04.17 12:11	in	-1,91	1,24	0,23				
29.04.17 12:19	in	-1,50	0,90	0,38				
29.04.17 13:06	in	-2,23	2,07	0,13				
29.04.17 13:12	in	-1,66	1,56	0,52				
29.04.17 13:19	in	-0,73	0,69	0,68				
29.04.17 14:06	in	-0,84	1,26	0,85				
29.04.17 14:13	in	-0,19	0,68	0,82				
29.04.17 15:06	in	-2,33	3,30	0,23				
29.04.17 15:13	in	-0,50	1,53	0,84				
29.04.17 15:18	in	0,46	0,61	0,84				
29.04.17 16:05	in	-0,51	1,98	0,84				
29.04.17 16:12	in	-0,09	1,62	0,78				
29.04.17 16:18	in	1,00	0,58	0,83				
29.04.17 16:53	in	-2,64	4,47	0,16				
29.04.17 16:59	in	-1,35	3,20	0,58				
29.04.17 17:05	in	0,96	0,93	0,56				

Supplement Table 5. Foraminiferal census data 2014, Esteiro Ancão do backbarrier beach transect

Sampling date: 30.04.2014

Counted specimens Station:	57	58	59	60	61	62	63	64	65	66	67	68	69	70	71	72
Section m:	47	43,5	41	39	37	34	31	28,5	26	24	21	17	13	10	7	3
Species Hight (m POD):	-0,87	-0,79	-0,77	-0,77	-0,76	-0,70	-0,60	-0,55	-0,47	-0,40	-0,29	0,07	0,41	0,73	1,03	1,53
Adelosina laevigata						3	5		5	1						
Adelosina longirostra		2						1								
Ammoglobigerina globigeriniformis			2		1	1	2									
Ammonia aberdoveyensis	7		4	5			1	2	1							
Ammonia beccarii		1														
Ammonia tepida	5	9	3	10		1	2	6		2		4				
Ammoscalaria runiana	40	22	20	8												
Asterigerinata mamilla	13	23	11	14	6	14	12	18	29	19	19	6				
Aubignyna hamblensis								1								
Bolivina italica		1	1		2	5	4	4		2	2	2				
Bolivina ordinaria	17	12	13	58	18	3	4	1	5	3	4	2	1			
Bolivina pseudoplicata		1	4	6	1	3	3	1	3							
Bolivina striatula	13	14	19	41	7	20	37	8	29	13	5	1				
Bolivina subaenariensis			1	2	2			2								
Bolivina variabilis			2													
Bulimina elegans		1	2	2												
Buliminella elegantissima	8	7	3	7	1	1	1									
Cassidulina minuta		1		1		1	1	1		1	1					
Cibicides lobatulus	3							3	5	2	5					
Cornuspira involvens				5		2	24	3		2						
Crithionina pisum			1	1												
Deuterammina balkwilli		1	3	3	6	8	9	5	10	10	7	26	17	4	7	
Deuterammina eddystonensis							4		2							
Deuterammina rotaliformis						3	11									
Eggerella europea	3	2														
Eggerelloides scaber	19	9	8	4	1		1									
Elphidium complanatum								1								
Elphidium cuvillieri				4	1		1									
Elphidium gerthi		2	1				2			2	1	1				
Elphidium williamsoni	6	2	7	10	6	2	4	2	2	2	10	11				
Epistominella vitrea	1						1									
Fissurina lucida			3		1			1								
Haynesina depressula	4	2	8	36	6	20	81	45	66	69	105	87	1			
Haynesina germanica	2	11	3	8	4	2	1	2	2	1	10	2				
Hopkinsina pacifica	1															
Jadammina macrescens	1			1												
Labrospira jeffreysii			1				2									
Lepidodeuterammina ochracea	2		6		4	6	16	1	4	7	2	1			1	
Leptohalysis scotti	1		4	1												
Miliammina fusca	2	2		1												
Miliolinella circularis												1				
Miliolinella hauerinoides	2		4	3		2						1	4			
Morulaeplecta bulbosa	8	3		3			2	1								
Neoconorbina terquemi		2	2			5	6	10	6	3	3	6				
Nonion fabum		1		2												
Patellina corrugata							1									
Portatrochammina haynesi				2	3			5			1					
Portatrochammina murrayi							2									
Quinqueloculina bicornis												2				
Quinqueloculina bosciana	13	13	18	57	6		15		9	8						
Quinqueloculina lata	1			2	2	2	4	1		3	4					
Quinqueloculina laevigata						8		4								
Quinqueloculina limbata		4	1	1		1	3	1	5	3	4					
Quinqueloculina parvula	2	6	9	20	5		3	9	6	1	4	3				
Quinqueloculina rugosa				3												
Quinqueloculina seminulum	4	3	7	28	7	9	21	30	36	11	88	13	2			
Quinqueloculina stelligera			1					1								
Rectuvigerina phlegeri	1	1			2		1	1		1						
Remaneica plicata				5												
Reophax arctica	25	3	12													
Reophax moniliformis	6	2		2												
Reophax nana	16	8	27	17	2											
Rosalina bradyi					1	1	2	1	3	4	5					
Rosalina globularis												6	2	1	1	
Rosalina vilardeboana	5	5	1	3	14	5	21	22	43	40	20	1	1			
Spirillina vivipara								1					2		1	
Stainforthia fusiformis				2												
Textularia earlandi	5		14	2												
Triloculina trigonula		1														
Trochamminita astrifica			2				1	1		1		1	2	1	4	
Wiesnerella auriculata	3		2				10	10	29	35	18					
others	2	3	8	6	4	7	12	7	7	4		2				
Total	241	180	238	386	113	135	333	213	307	250	318	179	32	6	14	0
Species no., counted	34	35	41	41	28	28	42	40	25	29	21	22	9	3	5	0
Sample volume (cm^3)	26,5	37	22	25	24	25	26	28,5	24	32,5	26,5	29	23	20	19	17
Split (n)	1	1	1	1	1	0,438	0,5	0,25	0,25	0,25	0,25	1	1	1	1	1
Population density (Ind./10 cm^3)	91	49	108	154	47	123	256	299	512	308	480	62	14	3	7	0
Fisher alpha index	10,8	13,0	14,3	11,6	11,9	10,7	12,7	14,6	6,4	8,5	5,1	6,6	4,2	2,4	2,8	0

Supplement Table 6. Foraminiferal census data 2015, Esteiro do Ancão backbarrier beach transect.

Sampling date: 20.04.2015

Counted specimens Station:	85	86	87	88	89	90	91	92	93	94	95	96	97	98	99
Section m:	45	40	36,8	33,5	29,9	26,5	23,7	19,8	16,1	14,2	12,7	11	9,2	8	3,1
Species Hight (m POD):	-0,93	-0,88	-0,87	-0,81	-0,67	-0,51	-0,38	-0,23	0,07	0,28	0,42	0,61	0,85	0,97	1,39
Adelosina laevigata	8	1		15	6										
Ammoglobigerina globigeriniformis				1											
Ammonia tepida	17	45	3	1	3		2		4	3					1
Ammoscalaria runiana	7	14			1										
Asterigerinata mamilla	5	8	12	16	25	26	30	6	1						
Aubignyna hamblensis	1	6	3	1							1				
Bolivina italica			1		7	2	1	7							
Bolivina ordinaria	8	13	6	2			2	2		1					
Bolivina pacifica		3					3								
Bolivina striatula	14	17	27	19	16	11	22	29							
Bolivina tongi		2		2	2		2								
Bolivina variabilis	2	2		2		2			1	1					
Bulimina elegans	3	3													
Bulimina marginata		6			1										
Buliminella elegantissima	3	8	2												
Cassidulina minuta				1		1		1							
Cornuspira involvens	1	1	2	3	5	2	1								
Crithionina granum					2			1				1			
Crithionina mamilla			1		2										
Deuterammina balkwilli			1	2	5	2	7	5	21	5	11		1		1
Deuterammina rotaliformis		1													
Eggerella europea	3				1										
Eggerelloides scaber	1	2													
Elphidium cuvillieri	13	21	2	7			2								
Elphidium excavatum					1		1	1							
Elphidium williamsoni		4	2	1			1	2							
Fissurina lucida	2	3	1		3	1		1							
Glabratella wrightii				1	2	1			3	2					
Glomospira gordialis							1								
Guttulina communis				4			1								
Haynesina depressula	4	40	31	9	23	13	38	88	14	7	2				
Haynesina germanica	18	14	2	2	3	3	2	3	4						
Hopkinsina pacifica	1	2													
Jadammina macrescens	1			1											
Lamarckina haliotidea					1										
Lenticulina atlantica				6	1										
Lepidodeuterammina ochracea	1		7	4	10	5	5	3	3						
Leptohalysis scotti	1	10													
Miliammina fusca	2	2													
Miliolinella hauerinoides	5	8										1			
Miliolinella hybrida					1										
Mississippina concentrica				1	2										
Morulaeplecta bulbosa		2													
Neoconorbina terquemi	1	3	2	4	9	11	11	7	2						
Nonionella iridea	4				1										
Patellina corrugata				1	4	1									
Portatrochammina haynesi								1							
Quinqueloculina bosciana	13	13	12	17	10	6	11	7							
Quinqueloculina lata						1	1		1						
Quinqueloculina limbata	3	5	2	1	4		2	4	1						
Quinqueloculina laevigata			1	3		1		15							
Quinqueloculina parvula	12	12	1	1	2	1	1	1							
Quinqueloculina seminulum	18	13	46	33	23	12	27	48	9	1	4	1			
Quinqueloculina stelligera			1	1											
Rectuvigerina phlegeri				2	1										
Remaneica helgolandica	2	1													
Remaneica plicata					1										
Reophax arctica	2	8													
Reophax nana	1	9			1										
Rosalina bradyi		2		1	3	2	2		2						
Rosalina cf. neapolitana							2	2							
Rosalina globularis									4		1	3	1	2	7
Rosalina vilardeboana		4	10	10	32	15	16	21	2	2	1				
Siphonaperta quadrata					1										
Spirillina vivipara			1	3	3		1	4	2	1	3	6			
Spirorbina sp.					2	2	3	3	8						
Stainforthia fusiformis	2	2													
Textularia earlandi	3	5													
Triloculina oblonga		1					3	3	2	1	1				
Trochammina inflata									2						2
Trochammina squamata			1				1	1	1						
Trochamminita astrifica					2				4		1	2		1	
Trochamminita irregularis									1						
Wiesnerella auriculata	1	1	2		8	7	3	2		1					
others	1	4		3	3	3	1		3						
Total	184	321	182	181	233	131	206	268	95	25	25	14	2	3	11
Species no., counted	36	43	27	35	43	25	32	27	24	11	9	6	2	2	4
Sample volume (cm^3)	31	27	33	27,5	22,5	23	35	26,5	27	19	28	20	25	21	25
Split (n)	0,125	0,30	0,13	0,13	0,25	0,13	0,13	0,25	1	1	1	1	1	1	1
Population density (Ind./10 cm^3)	475	400	441	527	414	456	471	405	35	13	9	7	1	1	4
Fisher alpha index	13,4	13,4	8,8	12,9	15,5	9,2	10,6	7,5	10,3	7,5	5,0	4,0		2,6	2,3

Supplement Table 7. Foraminiferal census data 2016, Esteiro do Ancão backbarrier beach transect.

Sampling date: 5.5.2016

Counted specimens Station:	115	116	117	118	119	120	121	122	123	124	125	126	127	128	129
Section m:	43	39	36	35,1	33,5	30	26,3	22	18,2	14,7	11,2	8	4	1,4	0,1
Species Hight (m POD):	-0,82	-0,78	-0,85	-0,85	-0,80	-0,68	-0,51	-0,33	-0,10	0,20	0,57	0,89	1,29	1,55	1,77
Adelosina laevigata	2		1	3	2	1	1								
Ammonia tepida	63	41	9	1	10	1	1	1							
Ammoscalaria runiana	11	6													
Ammotium salsum	3		1												
Asterigerinata mamilla	18	25	18	45	141	71	62	31	14	1					
Aubignyna hamblensis	11	5	4		2		1								
Bolivina italica					1	1									
Bolivina ordinaria	32	20	20	3	7	4	1	2	1						
Bolivina pacifica			1												
Bolivina striatula	22	27	11	4	14	5	5	16	1						
Bolivina tongi	1		1			1		4							
Bolivina variabilis	1	2	2	4	5	3		1	1						
Bulimina elegans	4	4	3												
Bulimina marginata		3	1												
Buliminella elegantissima	14	7	1	2											
Cassidulina minuta					1		1	3							
Cibicides lobatulus		1					4	1							
Cornuspira involvens	4		1	2	36	13	1								
Crithionina mamilla			1	1	2		2								
Deuterammina balkwilli				3		6		1	13	20	8				
Deuterammina rotaliformis	2														
Discorinopsis aguayoi											1				
Eggerella europea				1											
Eggerelloides scaber	10	6	2												
Elphidium crispum									1						
Elphidium cuvillieri	7	4	13		1										
Elphidium gerthi							3	5	1						
Elphidium williamsoni	7	6	9	2	5	1	2	1	1	1					
Fissurina lucida	2	1	1	1	1		2								
Glabratella wrightii					1			8							
Guttulina communis						1	1								
Haynesina depressula	28	28	13	45	93	39	48	51	134	3	1				
Haynesina germanica	19	14	8	3	6	2	1	2	1						
Hopkinsina pacifica	3														
Jadammina macrescens														2	1
Lenticulina atlantica					2	2									
Lepidodeuterammina ochracea		2	1	1	2	1	11	2							
Leptohalysis scotti	9	3													
Miliammina fusca	4	1			1										
Miliolinella hauerinoides	8	1	14		4	2		1							
Neoconorbina terquemi		1	2	6	14	7	11	1	1						
Nonionella iridea	1														
Patellina corrugata				1	6	3	1	1		2	2				
Portatrochammina haynesi							2	1	1		2	1			
Quinqueloculina bosciana	37	13	10	5	11	5	4	13	5	3					
Quinqueloculina limbata	9	7	6	2	3			5	2						
Quinqueloculina laevigata			2	1				1	7						
Quinqueloculina parvula	6	5	5	3	2	2	2	1							
Quinqueloculina seminulum	39	61	32	21	66	22	11	22	9	2	4				
Rectuvigerina phlegeri							1								
Remaneica plicata				1											
Reophax arctica	8	4	1												
Reophax nana	27	7	2												
Rosalina bradyi											1				
Rosalina globularis											2	4	2	6	4
Rosalina macropora			1		1										
Rosalina vilardeboana	1	3		5	14	18	21	10	6	1					
Siphonaperta quadrata	2	7	15		1										
Spirillina vivipara					2										
Spirorbina sp.					7	13	5	8	2						
Textularia earlandi	2	4	1		2		1								
Triloculina oblonga										1					
Trochammina inflata	1			1						1				1	3
Trochammina squamata			1				1	1							
Trochamminita astrifica	1		1		4										
Wiesnerella auriculata				4	13	18	15	10	5						
others	1	7		1		4	3	1	2					1	
Total	420	326	215	172	483	246	225	205	208	35	21	5	2	10	8
Species no., counted	37	34	36	28	35	28	31	29	20	10	8	2	1	4	3
Sample volume (cm^3)	31	28	25	18,5	26	19	25	35	22,5	20	19	22,5	20	22	21
Split (n)	0,125	0,13	0,12	0,13	0,25	0,13	0,13	0,13	0,5	1	1	1	1	1	1
Population density (Ind./10 cm^3)	1084	931	710	744	743	1036	720	469	185	18	11	2	1	5	4
Fisher alpha index	9,8	9,6	12,4	9,5	8,7	8,1	9,7	9,2	5,5	4,7	4,7	1,2	-	2,5	1,7

Supplement Table 8. Foraminiferal census data 2017, Esteiro do Ancão backbarrier beach transect.
Sampling date: 25.4.2017

Counted specimens Station:	146	147	148	149	150	151	152	153	154	155	156	157	158	159
Section m:	43	40	36	34	30,5	26	23	18,5	15	13	11	9	4	1
Species Hight (m POD):	-0,80	-0,78	-0,76	-0,80	-0,67	-0,49	-0,36	-0,13	0,19	0,40	0,60	0,78	1,17	1,58
Adelosina laevigata				5	11									
Adelosina longirostra				5										
Ammonia aberdoveyensis								1						
Ammonia tepida	3	4	8					7	2					
Ammoscalaria runiana	5	5	3											
Ammotium salsum	1		1	1	3			1						
Asterigerinata mamilla	26	21	21	41	38	71	74	22	3					
Aubignyna hamblensis	1	1	3	1										
Bolivina dilatata			1											
Bolivina italica				12	24	1	5							
Bolivina ordinaria	5	7	7	16	1	6	8	3	2	1				
Bolivina pacifica	1	2	3											
Bolivina striatula	8	8	23	21	17	3	7	1						
Bolivina tongi			1	1	4	2								
Bolivina variabilis	1	4	9	6	8	4	3							
Buliminella elegantissima	4	2	4			1								
Cassidulina minuta				1	5	1	2							
Cibicides lobatulus				1			1							
Cornuspira involvens		5		63	32	1	2							
Crithionina mamilla	3		3	7		8	1							
Deuterammina balkwilli			2	6	1	9	4	12	28	18				
Deuterammina rotaliformis				8										
Discorinopsis aguayoi									2	2				
Eggerelloides scaber	9	10	12	3	1									
Elphidium cuvillieri						2								
Elphidium gerthi		2	3	1	1									
Elphidium williamsoni	1	7	4						1					
Fissurina lucida	2													
Glabratella wrightii	1			1	2		1	5		1				
Guttulina communis				7	9									
Haynesina depressula	6	3	7	9	5	6	28	38	2					
Haynesina germanica	1		5		1		2	1						
Hopkinsina pacifica			1											
Jadammina macrescens	1		1					1			1		1	
Labrospira jeffreysii			1	2	2		2							
Lenticulina atlantica				4	2		1							
Lepidodeuterammina eddystonensis						1	1	1						
Lepidodeuterammina ochracea	1		2	6	8	5	3	2						
Leptohalysis scotti	3	2	1	1										
Miliammina fusca		1												
Miliolinella hauerinoides	2			3	1	1								
Morulaeplecta bulbosa	6	5	2	1										
Neoconorbina terquemi		1		3	3	35	33	1						
Nonionoides grateloupii				2										
Patellina corrugata					1									
Planorbulina mediterranensis						6								
Portatrochammina haynesi	1		2	2	2	2	2	7	7	5			1	
Quinqueloculina bosciana	11	1	3	3	19	10	23	3						
Quinqueloculina limbata				2			3	1						
Quinqueloculina laevigata		1	13	31										
Quinqueloculina parvula	1		2	1										
Quinqueloculina seminulum	4	5	6	7	11	12	25	20	1	1			1	
Rectuvigerina phlegeri	1		1	1	7		1							
Reophax arctica	10	12	13											
Reophax nana	68	75	73	5	2		1							
Rosalina bradyi				1	2		4	6	7	3	3	1		
Rosalina globularis									2	4	1		5	
Rosalina macropora				5	1	3								
Rosalina vilardeboana			4	9	23	11	19	2						
Saccammina sphaerica	1													
Siphonaperta quadrata					2			3						
Spirillina vivipara					2	1	1			1				
Spirorbina sp.				2	1	24	6	2						
Textularia earlandi	3	4	13											
Trochammina advena	1	1	1	6										
Trochammina inflata				1		1		1			1		1	
Trochammina squamata				2	1	1								
Trochamminita astrifica	3	3	3		5									
Wiesnerella auriculata				3	1	4	2							
others	1	8	2		1	4	5	1	2				1	
Total	196	200	264	319	260	236	270	142	59	36	6	1	10	0
Species no., counted	34	28	38	45	39	30	31	24	12	9	4	1	6	0
Sample volume (cm^3)	38	31	34,5	30	27	26	29	28	24	25	23	18	26	25
Split (n)	0,5	1,00	1,00	1,00	0,63	1,00	0,25	1,00	1	1	1	1	1	1
Population density (Ind./10 cm^3)	103	65	77	106	154	91	372	51	25	14	3	1	4	0
Fisher alpha index	11,9	8,9	12,2	14,3	12,7	9,1	9,0	8,3	4,6	3,9	5,3	-	6,3	-

Supplement Table 9. Foraminiferal census data from the 30-m monitoring site.

Percentages	Station:	54		63		89		120		150		180		226	
	Sampling date:	15.4.2013		30.4.2014		20.4.2015		5.5.2016		25.4.2017		03.05.2018		8.5.2019	
	Section m:	30,2		31		29,9		30		30,5		30,5		30,5	
	Hight (m POD):	-0,61		-0,60		-0,67		-0,68		-0,67		-0,68		-0,71	
Species	Assemblage:	living	dead	living	dead	living	dead	living	dead	living	dead	living	dead	living	dead
Adelosina laevigata				1,50	1,7	2,58	1,1	0,41	1,5	4,23		1,82		1,20	
Ammoglobigerina globigeriniformis				0,60	0,6										
Ammonia aberdoveyensis				0,30							1,0				
Ammonia tepida		3,6	3,7	0,6	4,6	1,3	7,5	0,4	16,2		6,0		5,9		4,1
Ammoscalaria runiana						0,4									
Ammotium salsum										1,2		1,2		0,8	
Asterigerinata mamilla		6,4	21,9	3,6	15,5	10,7	9,1	28,9	11,8	14,6	11,6	24,2	28,2	13,8	20,0
Aubignyna hamblensis					1,2		1,1								1,4
Bolivina dilatata		0,9													0,7
Bolivina italica		2,7	1,0	1,2	0,6	3,0	1,1	0,4		9,2		1,2		5,7	
Bolivina ordinaria		9,1	1,6	1,2	0,6		1,6	1,6		0,4	2,0	4,8	1,1	1,6	1,4
Bolivina pseudoplicata		4,5	0,5	0,9									0,4		
Bolivina striatula		1,8	3,7	11,1	1,7	6,9	2,2	2,0		6,5	4,0	3,6	1,8	5,7	2,8
Bolivina tongi			0,5			0,9		0,4	2,9	1,5	0,5	0,6		1,6	0,7
Bolivina variabilis							1,1	1,2		3,1	1,5	4,2	1,1	1,6	2,1
Bulimina marginata						0,4									
Buliminella elegantissima				0,3								0,6			
Cassidulina laevigata			0,5												
Cassidulina minuta				0,3	0,6		1,1			1,9	0,5	0,6	0,7	2,0	2,8
Cibicides lobatulus		0,9	10,4		14,9		18,8		11,8		20,6		9,5		9,7
Cornuspira involvens				7,2	4,6	2,1	1,6	5,3		12,3	5,0	6,1	0,4	10,6	
Crithionina granum						0,9									
Crithionina mamilla						0,9						0,6		3,3	
Deuterammina balkwilli				2,7		2,1		2,4		0,4	1,0	3,0			
Deuterammina eddystonensis				1,2											
Deuterammina rotaliformis		2,7		3,3											
Discorinopsis aguayoi											0,5				
Eggerella europea						0,4									
Eggerelloides scaber				0,3						0,4				1,6	
Elphidium advenum			5,7		4,6						7,5		3,7		
Elphidium complanatum					1,2				1,5		1,0		0,4		
Elphidium crispum									7,4						6,9
Elphidium cuvellieri		0,9		0,3											
Elphidium excavatum		2,7				0,4									
Elphidium gerthi			6,8	0,6	2,3		3,8		4,4	0,4	3,0		4,0		2,8
Elphidium oceanensis							2,2		1,5				1,5		0,7
Elphidium poeyanum					2,3								0,4		
Elphidium williamsoni				1,2				0,4						0,8	
Epistominella vitrea				0,3											
Eponides repandus					0,6		0,5		2,9		1,0		0,7		0,7
Fissurina lucida						1,3								0,4	
Gavelinopsis praegeri							0,5				1,0		1,1		
Glabratella wrightii						0,9				0,8					
Guttulina communis							0,5	0,4		3,5					
Haynesina depressula		2,7	1,6	24,3	3,5	9,9	6,5	15,9	2,9	1,9	1,0	4,2	2,2	0,8	3,5
Haynesina germanica			2,1	0,3	0,6	1,3	1,1	0,8	4,4	0,4	1,5	1,2	2,2	0,4	1,4
Jadammina macrescens			0,5												0,7
Labrospira jeffreysii				0,6						0,8		0,6			
Lamarckina haliotidea						0,4									
Lenticulina atlantica						0,4		0,8		0,8	0,5				
Lenticulina rotulata					0,6										
Lepidodeuterammina eddystonensis											0,5				
Lepidodeuterammina ochracea		2,7	0,5	4,8		4,3		0,4		3,1	1,5	1,8		3,7	
Leptohalysis scotti		0,9													
Massilina gualtieriana			1,0												
Miliammina fusca		0,9													
Miliolinella hauerinoides			1,6				0,5	0,8		0,4	1,5		1,5		
Miliolinella hybrida						0,4									
Mississippina concentrica			0,5			0,9							0,7		
Morulaeplecta bulbosa				0,6											

Percentages	Station:	54		63		89		120		150		180		226	
	Sampling date:	15.4.2013		30.4.2014		20.4.2015		5.5.2016		25.4.2017		03.05.2018		8.5.2019	
	Section m:	30,2		31		29,9		30		30,5		30,5		30,5	
	Hight (m POD):	-0,61		-0,60		-0,67		-0,68		-0,67		-0,68		-0,71	
Species	Assemblage:	living	dead	living	dead	living	dead	living	dead	living	dead	living	dead	living	dead
Neoconorbina terquemi				1,8	0,6	3,9		2,8		1,2		1,2		8,5	4,8
Nonion fabum							1,1						0,4		
Nonionella bradyi		1,8													
Nonionella iridea						0,4									
Patellina corrugata				0,3		1,7		1,2		0,4					
Planorbulina mediterranensis			0,5		1,7						1,0		5,1		1,4
Portatrochammina haynesi										0,8	0,5			1,2	
Portatrochammina murrayi				0,6											
Quinqueloculina agglutinata					2,3		0,5		2,9		2,0		1,5		2,8
Quinqueloculina berthelotiana					0,6						0,5		0,4		
Quinqueloculina bosciana		13,6	3,1	4,5	4,0	4,3	2,2	2,0	1,5	7,3	2,5	9,7	2,9	10,6	2,1
Quinqueloculina laevigata		1,8	12,5		4,6		8,1		11,8		5,5		3,7	2,0	9,7
Quinqueloculina lata			0,5	1,2			1,1				1,0	1,82	0,7		
Quinqueloculina limbata			1,0	0,9	2,9	1,72			4,4		1,5		1,1	0,41	
Quinqueloculina parvula		0,9	0,5	0,9		0,9	1,1	0,8			0,5	0,6	2,2	1,6	2,1
Quinqueloculina seminulum		25,5	3,1	6,3	4,6	9,9	9,7	8,9	4,4	4,2	1,5	6,1	4,4	2,8	4,8
Quinqueloculina stelligera					1,2										
Rectuvigerina phlegeri			0,5	0,3		0,43				2,69		3,03		0,4	
Remaneica plicata						0,43									
Reophax arctica														0,4	
Reophax moniliformis		1,8													
Reophax nana						0,43				0,77		1,21		0,4	
Rosalina bradyi			3,1	0,6	0,6	1,29	1,6			0,8			1,5		2,1
Rosalina cf. *neapolitana*													0,4		
Rosalina globularis			0,5		1,2		0,5				1,5				
Rosalina macropora		1,8	3,1		4,0		3,8			0,4	3,0	2,4	1,1	2,0	2,8
Rosalina vilardeboana		1,8	2,6	6,3	6,9	13,7	6,5	7,3	4,4	8,8		4,8	2,9	4,1	1,4
Siphonaperta quadrata						0,43				0,77				2,4	
Spirillina vivipara						1,29				0,77				1,2	
Spirorbina sp.						0,86	1,1	5,28		0,38	1,0	1,82	1,8		2,1
Textularia pseudogramen					0,6								0,4		
Tiphotrocha comprimata		0,9													
Trochammina advena												0,61		0,4	
Trochammina inflata		0,9	0,5												
Trochammina squamata										0,38		1,21		0,4	
Trochamminita astrifica			0,5	0,3		0,86			1,5	1,92				2	
Wiesnerella auriculata		4,5		3,0	0,6	3,4		7,3		0,4		0,6	0,7		
others		0,9	3,7	3,6	1,7	1,3	1,1	1,6		0,4	3,5	4,2	1,5	3,3	2,1
Total counted specimens		110	192	135	174	233	186	246	68	260	199	165	273	246	145
Abundance (Ind./10 cm^3)		100	706	256	360	414	538	1036	286	154	295	122	532	79	391
Fisher alpha		11,4	12,5	12,7	14,4	15,5	11,7	8,1	8,7	12,7	15,1	14,2	12,9	13,8	12,1

Supplement Table 10. Nutrient measurements of Esteiro do Ancão surface waters.

Year	Date	Time	Tide	location	Nitrate (μmol l^{-1})	Phosphate (μmol l^{-1})
2017	11.04.17	10:15	ebb	Aeromar slipway	0,512	0,277
	22.04.17	18:05	ebb	Aeromar slipway	12,851	0,305
	23.04.17	18:12	ebb	Aeromar slipway	15,955	0,555
	26.04.17	08:20	ebb	Aeromar slipway	1,479	0,228
	29.04.17	11:25	ebb	Aeromar slipway	6,826	0,627
2018	04.05.18	10:05	ebb	Ponte da Praia de Faro	6,152	0,219
	06.05.18	12:20	ebb	Ponte da Praia de Faro	0,336	0,326
	08.05.18	12:35	ebb	Ponte da Praia de Faro	1,713	0,714
2019	02.05.19	07:40	ebb	Ponte da Praia de Faro	< 0,01	0,373
	05.05.19	08:20	ebb	Ponte da Praia de Faro	< 0,01	0,328
	07.05.19	10:20	ebb	Ponte da Praia de Faro	< 0,01	0,336
	09.05.19	11:55	ebb	Ponte da Praia de Faro	< 0,01	0,308
				Mean 2017:	7,525	0,398
				Mean 2018:	2,734	0,420
				Mean 2019:	< 0,01	0,336